APPENDICES

APPENDIX A1 - Stress-strain graphs of UCS tests of BRPM and Khomanani Platinum mines

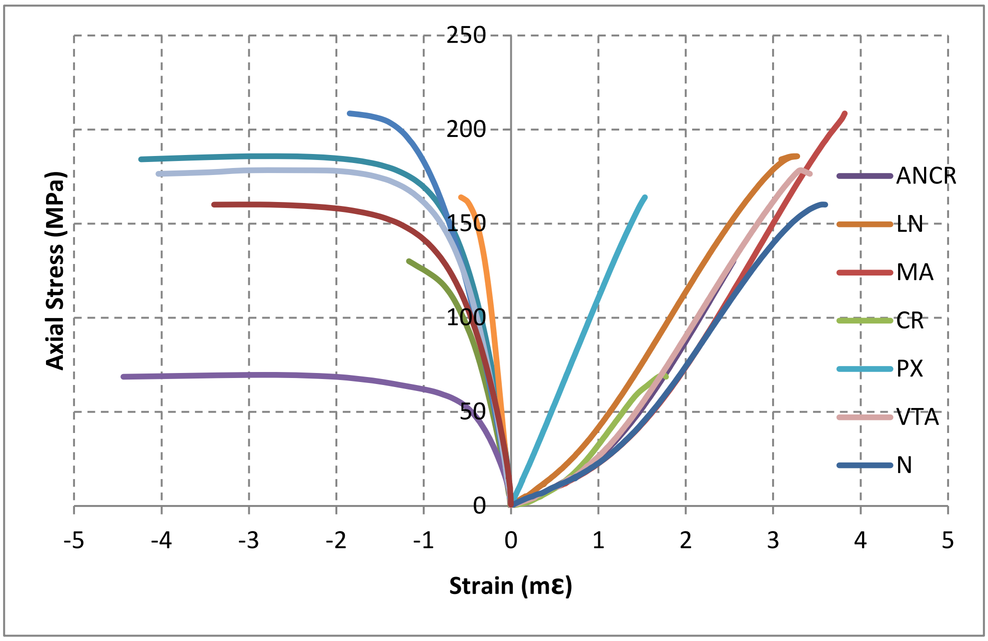

Figure A1 1: Stress-strain plot for BRPM uniaxial compressive strength tests

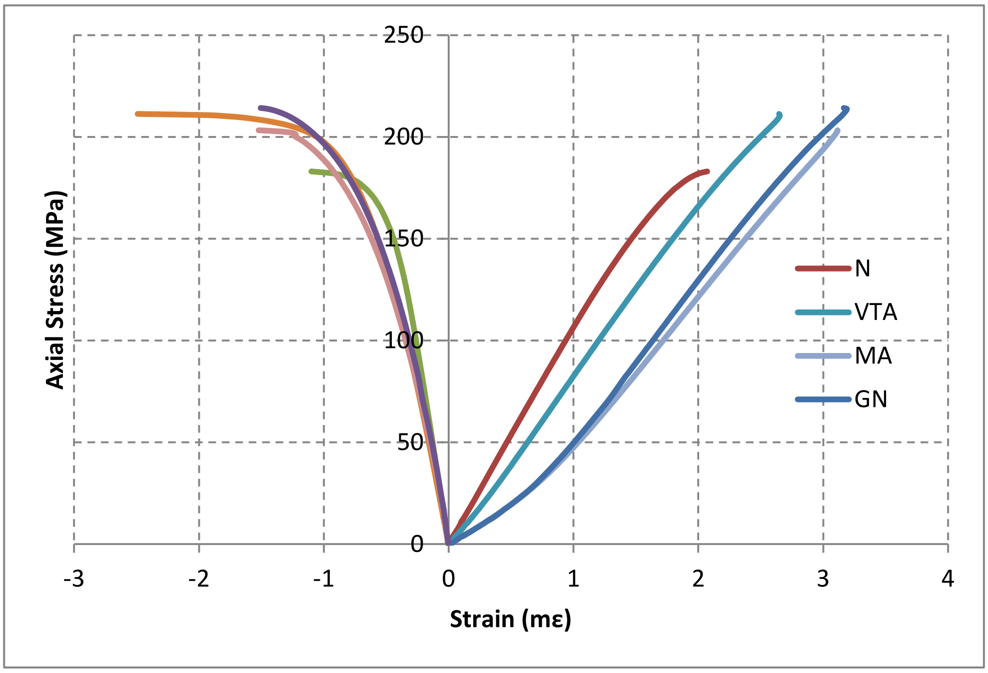

Figure A1 2: Stress-strain plot for Khomanani uniaxial compressive strength tests

APPENDIX A2 – The results of the confined thermal expansion tests

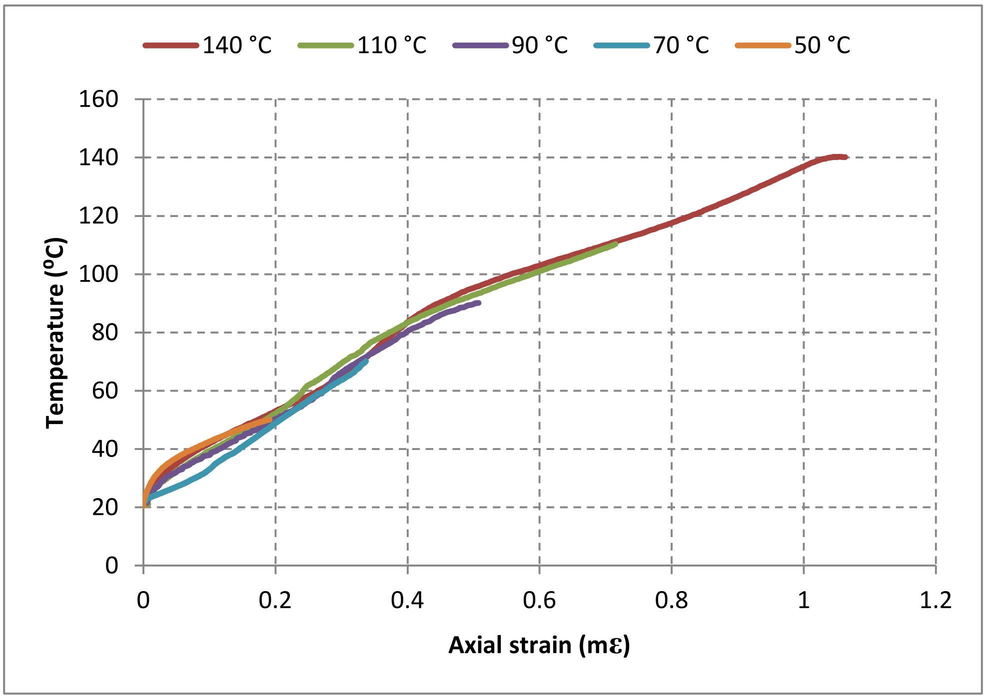

Figure A2 1: Temperature versus axial strain for anorthosite-chromitite

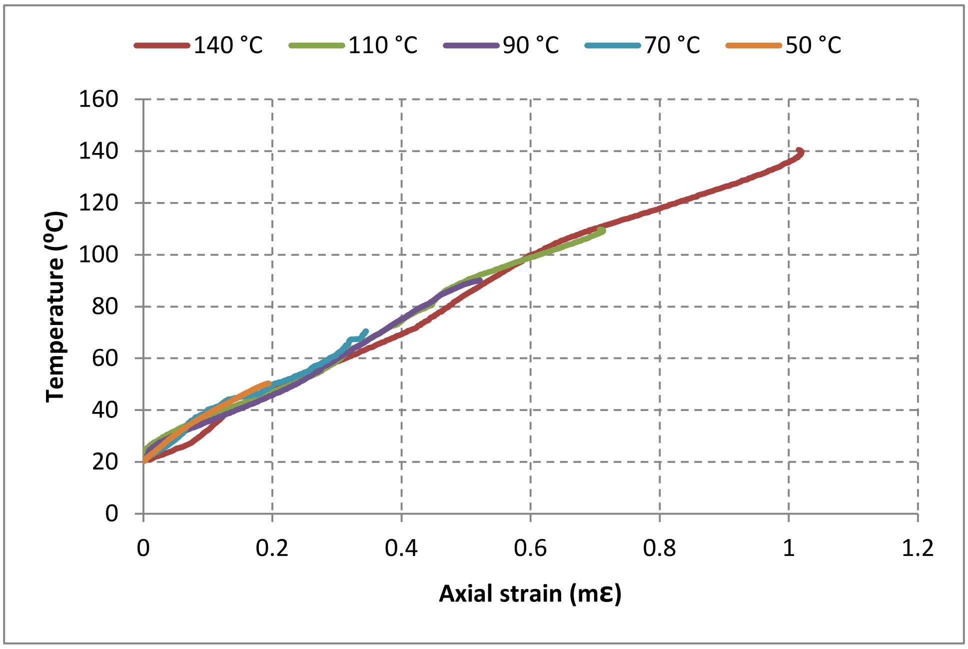

Figure A2 2: Temperature versus axial strain for chromitite

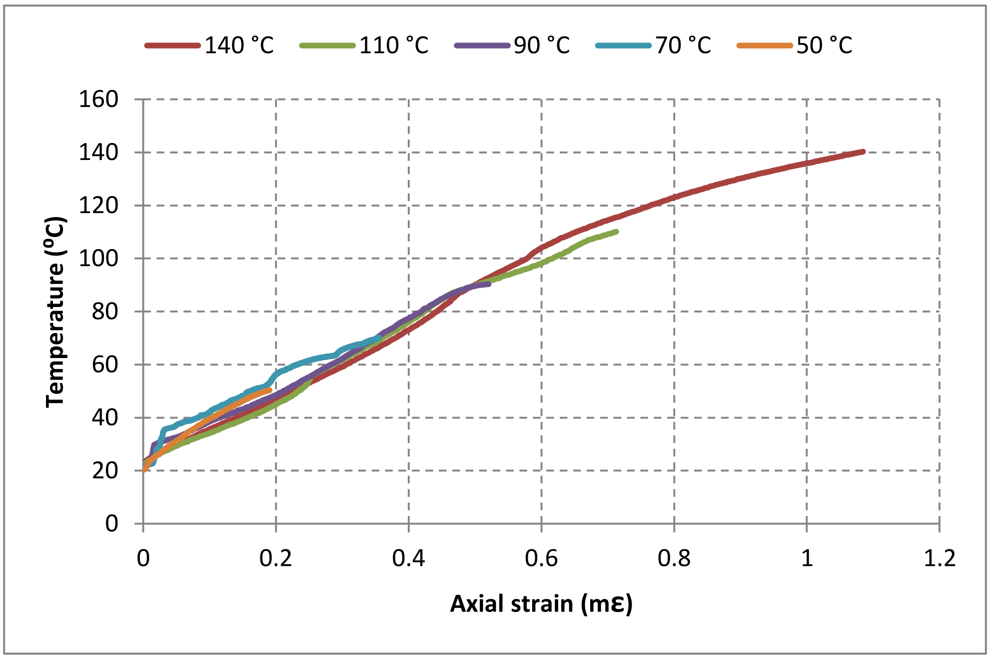

Figure A2 3: Temperature versus axial strain for vari-textured anorthosite

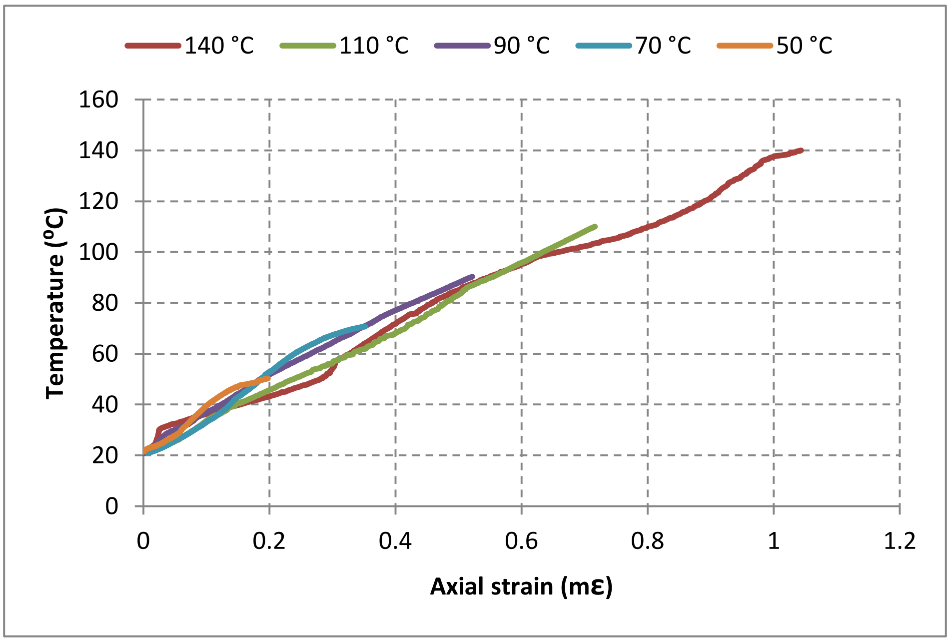

Figure A2 4: Temperature versus axial strain for pyroxenite

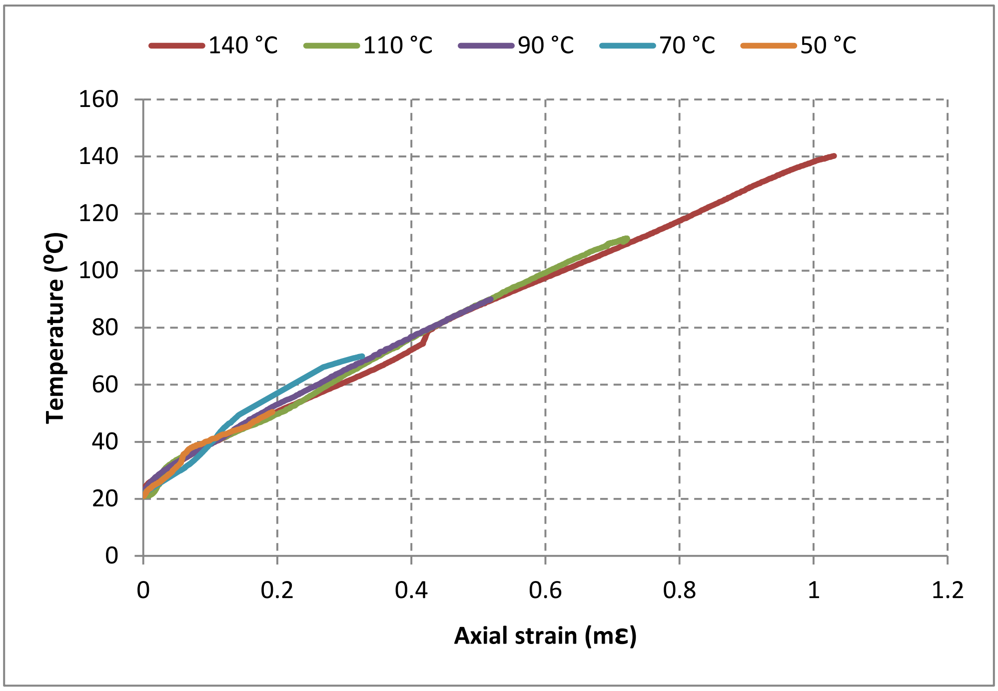

Figure A2 5: Temperature versus axial strain for leuconorite

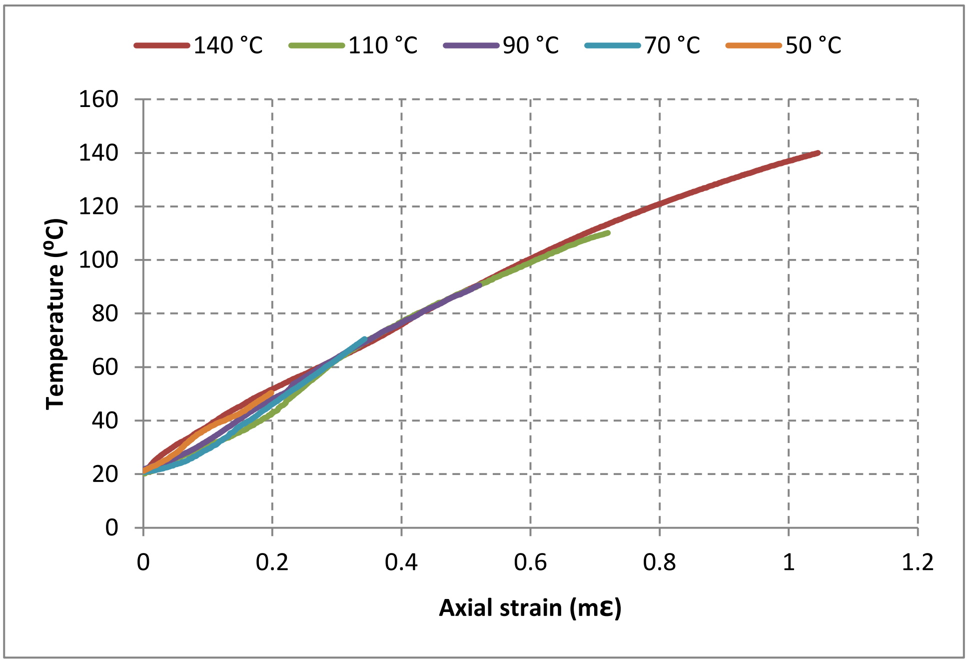

Figure A2 6: Temperature versus axial strain for mottled anorthosite

APPENDIX A3 – The results of the temperature-compression tests with MTS servo-control testing machine.

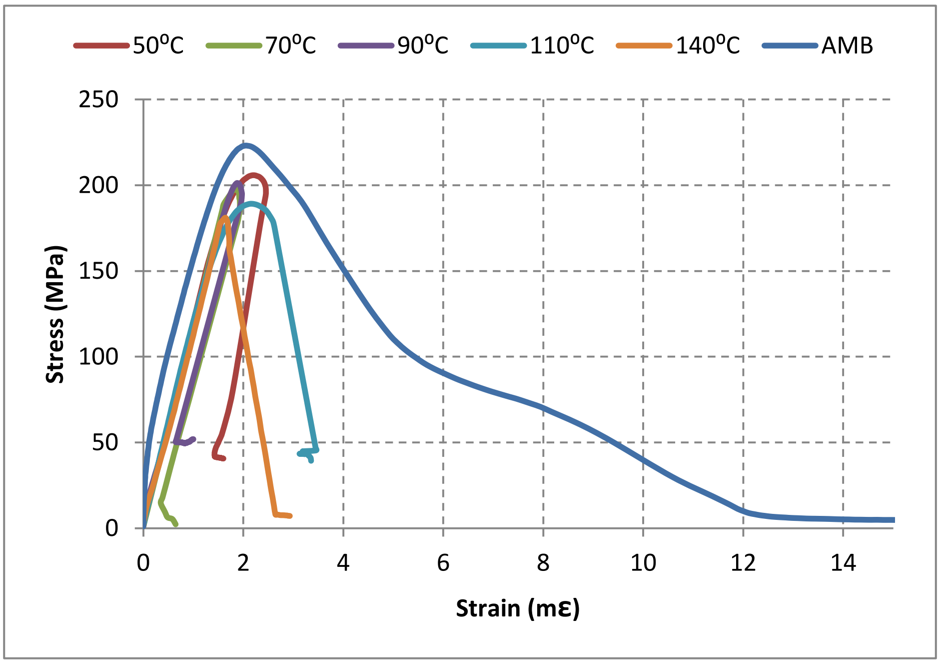

Figure A3 1: Pyroxenite tested at 10 MPa confinement, different temperatures

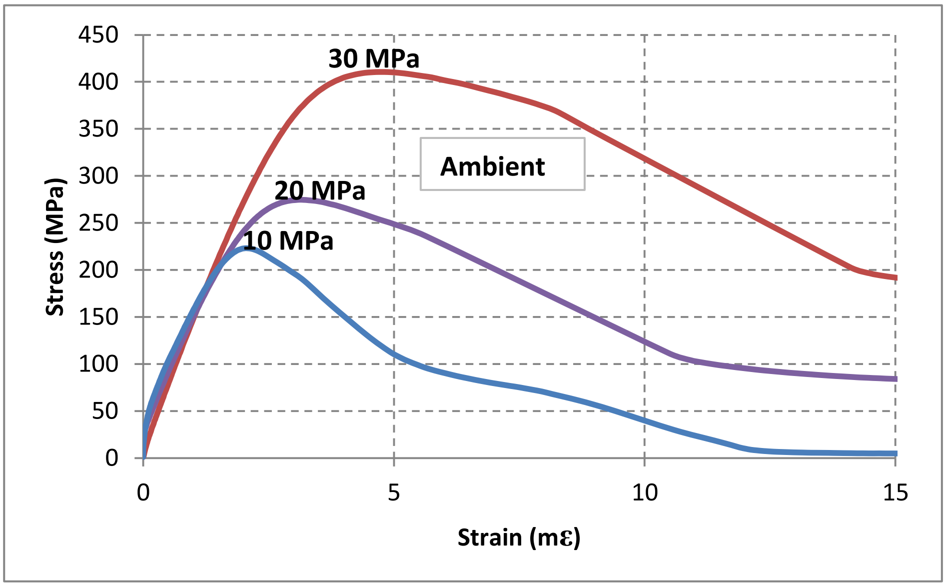

Figure A3 2: Pyroxenite tested at ambient temperature, different confinements

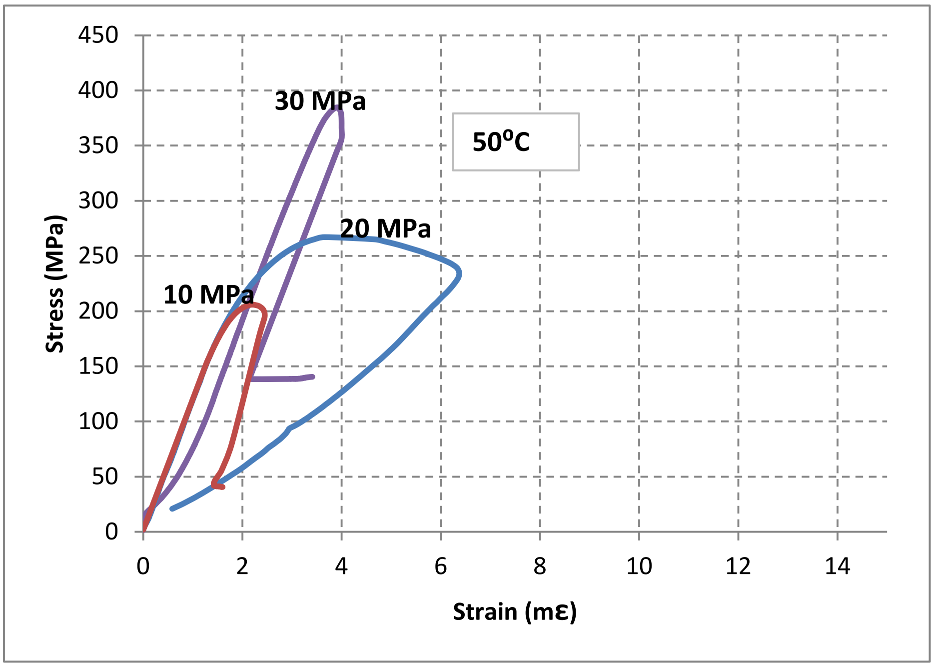

Figure A3 3: Pyroxenite tested at 50°C, different confinements

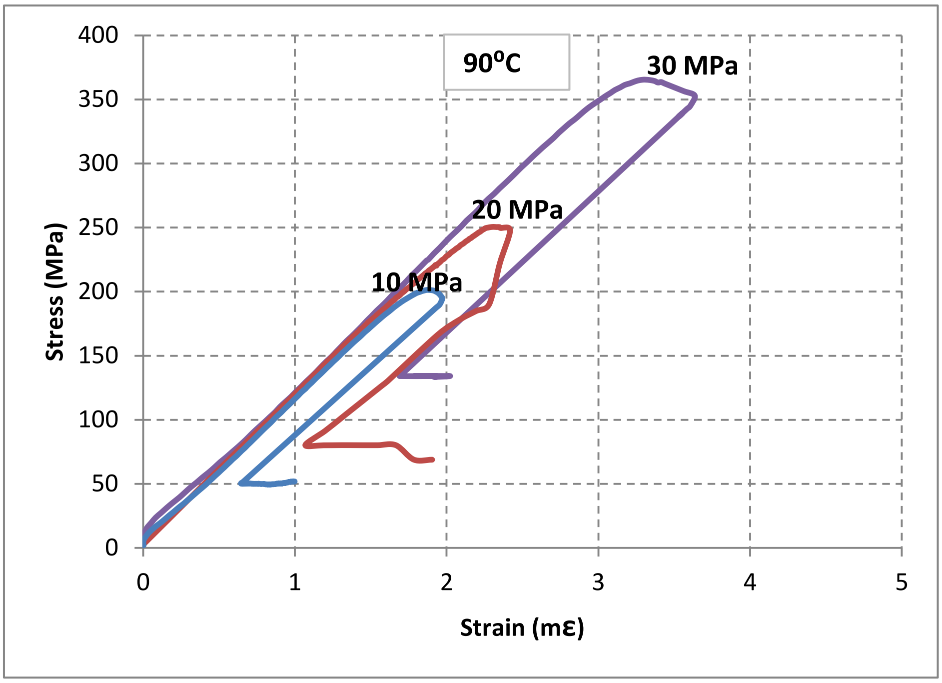

Figure A3 4: Pyroxenite tested at 90°C, different confinements

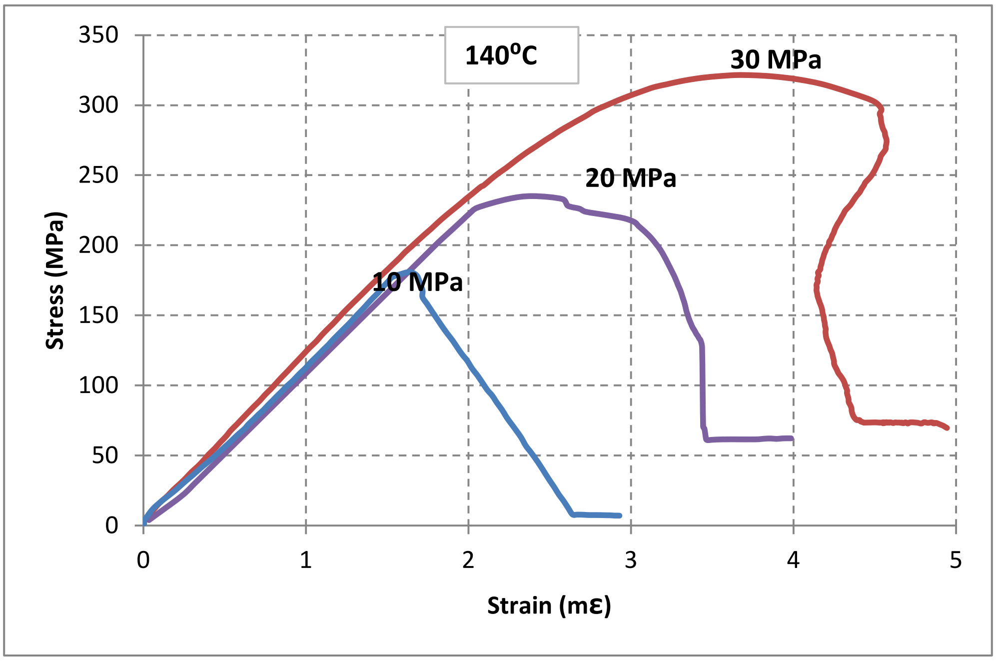

Figure A3 5: pyroxenite tested at 140°C, different confinements

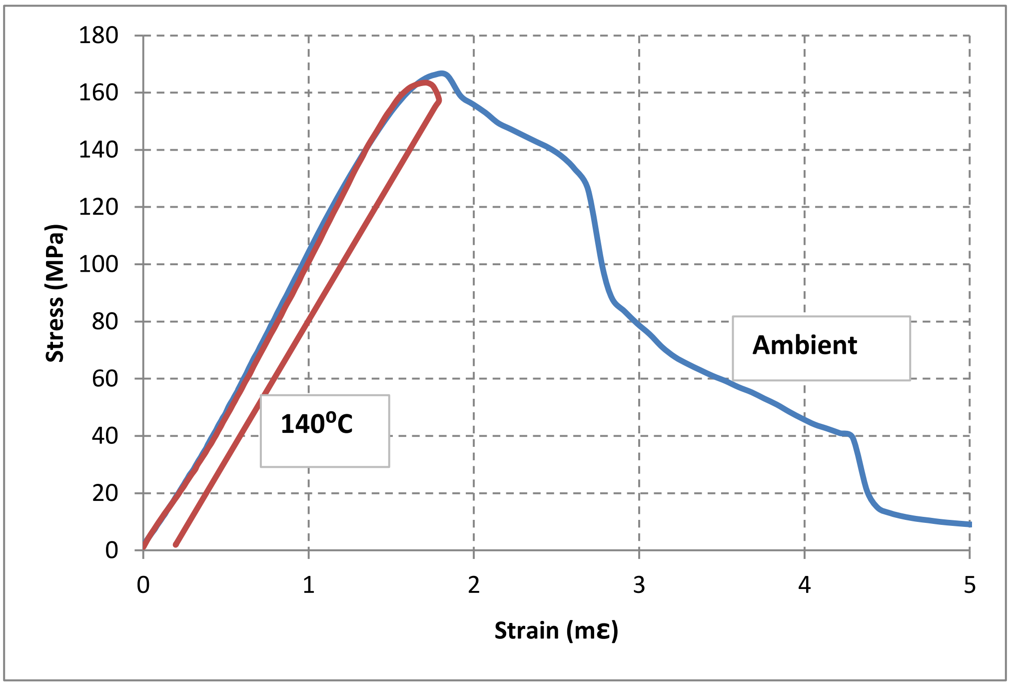

Figure A3 6: Pyroxenite tested at ambient and 140°C, zero confinement

Table A3 1: Young's Modulus and Poisson's Ratio of pyroxenite

	AMB	50°C	70°C	90°C	110°C	140°C
			Young's modulus (GPa)			
0 MPa	112.0					109.0
10 MPa	121.0	118.6	116.9	114.8	113.2	112.9
20 MPa	121.2	119.2		117.4		114.8
30 MPa	122.6	120.6		119.0		113.8
			Poisson's Ratio			
0 MPa	0.24					0.24
10 MPa	0.24	0.24	0.24	0.24	0.25	0.24
20 MPa	0.24	0.25		0.24		0.25
30 MPa	0.25	0.25		0.25		0.24

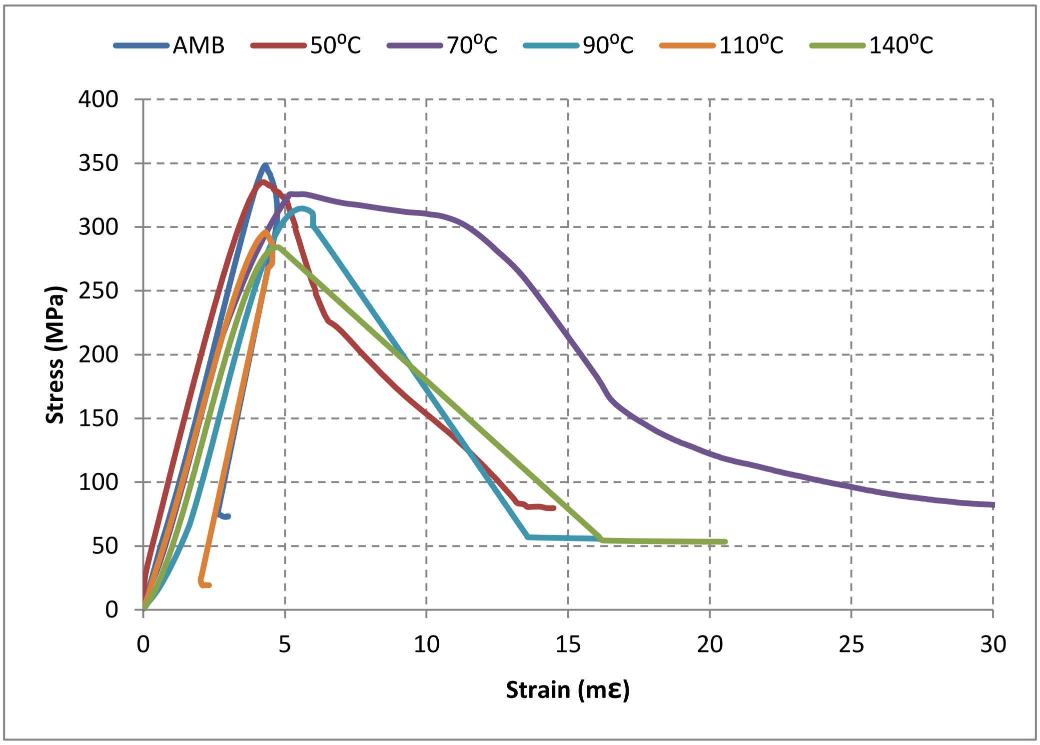

Figure A3 7: Mottled anorthosite tested at 10 MPa confinement, different temperatures

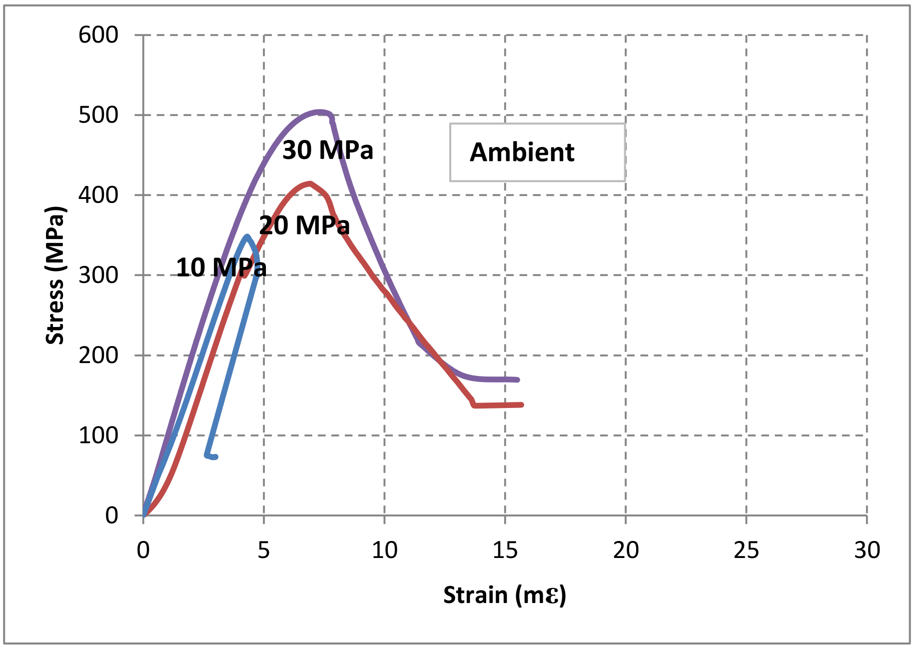

Figure A3 8: Mottled anorthosite tested at ambient temperature, different confinements

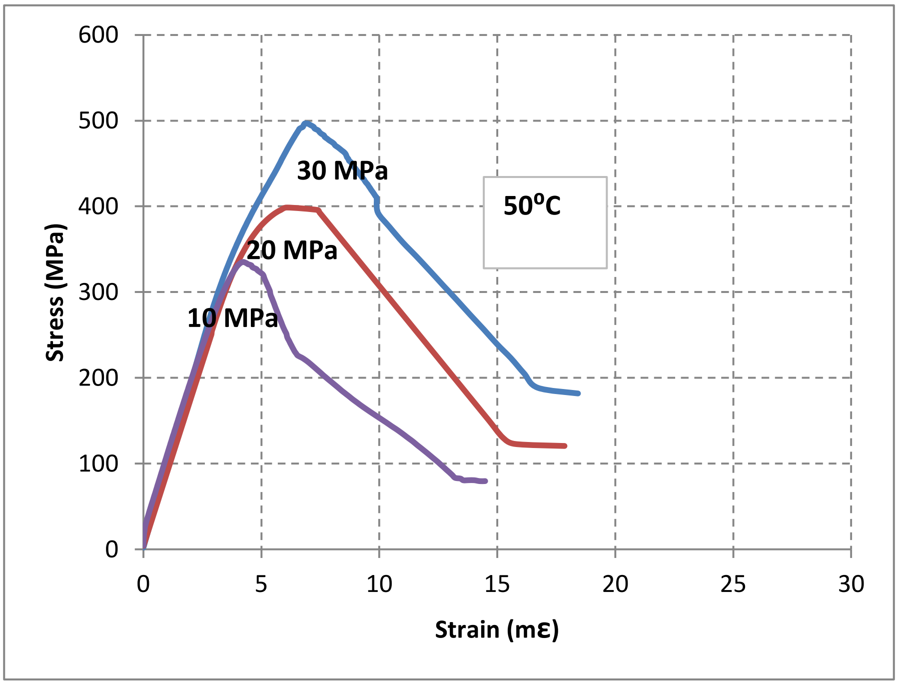

Figure A3 9: Mottled anorthosite tested at 50°C, different confinements

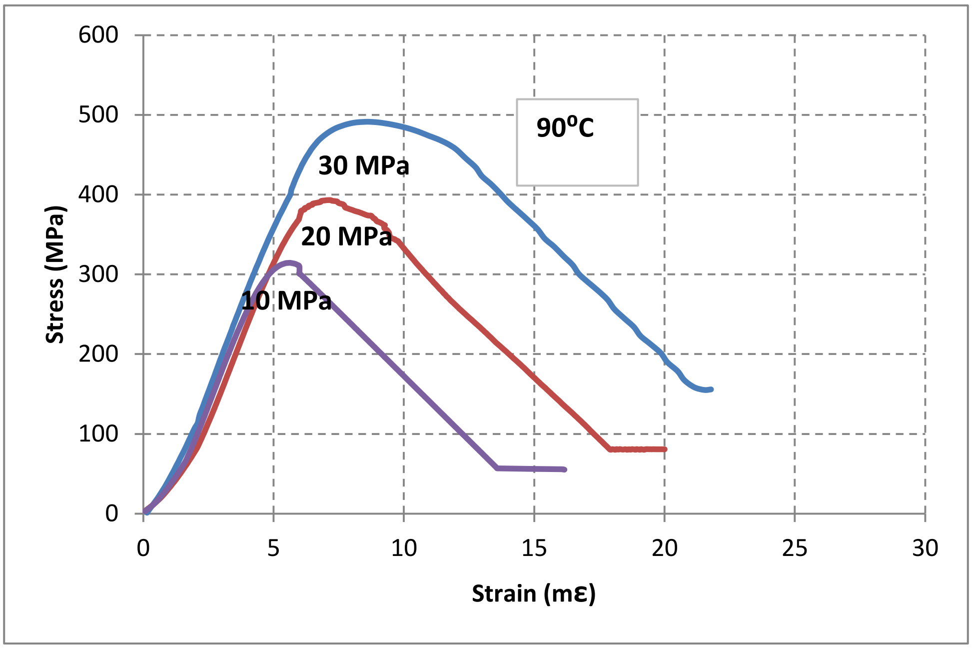

Figure A3 10: Mottled anorthosite tested at 90°C, different confinements

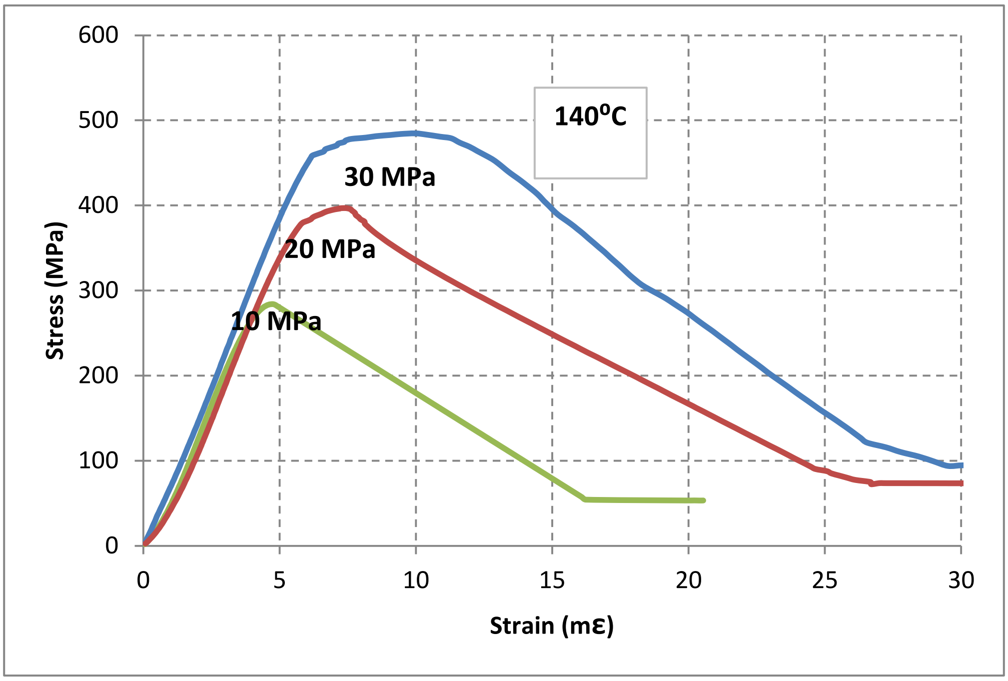

Figure A3 11: Mottled anorthosite tested at 140°C, different confinements

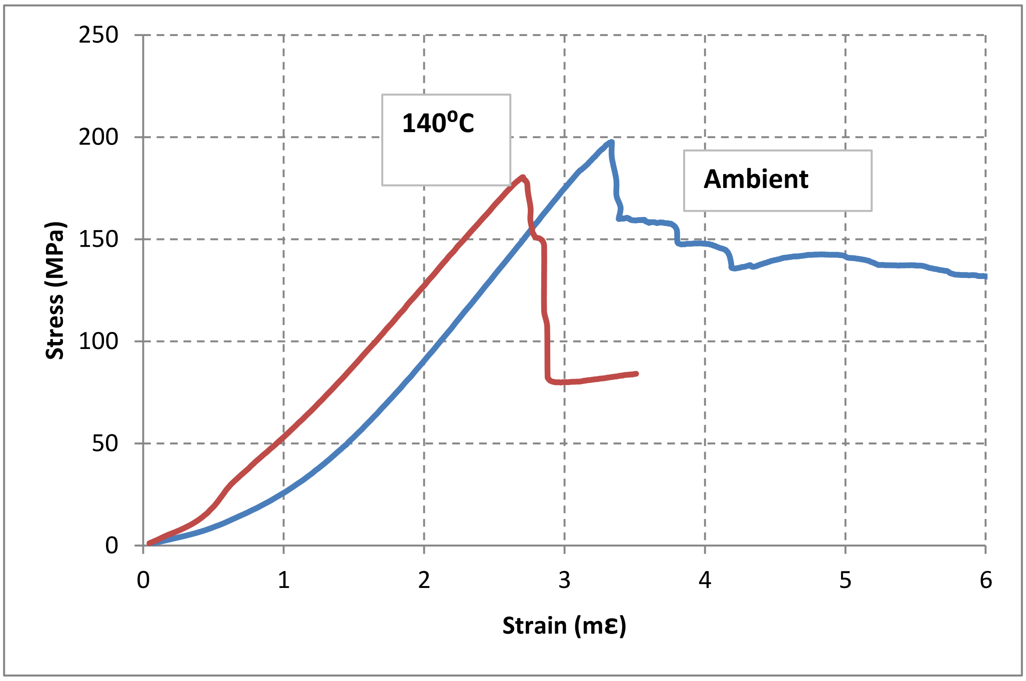

Figure A3 12: Mottled anorthosite tested at ambient and 140°C, zero confinement

Table A3 2: Young’s modulus and Poisson's Ratio of mottled anorthosite

	AMB	50°C	70°C	90 °C	110°C	140°C
			Young’s modulus (GPa)			
0 MPa	80.9					75.1
10 MPa	87.1	84.7	83.8	82.9	81.6	79.9
20 MPa	89.8	85.7		83.5		81.5
30 MPa	90.5	88.4		84.1		82.3
			Poisson’s Ratio			
0 MPa	0.35					0.36
10 MPa	0.37	0.36	0.37	0.36	0.37	0.36
20 MPa	0.36	0.36		0.36		0.36
30 MPa	0.37	0.36		0.36		0.35

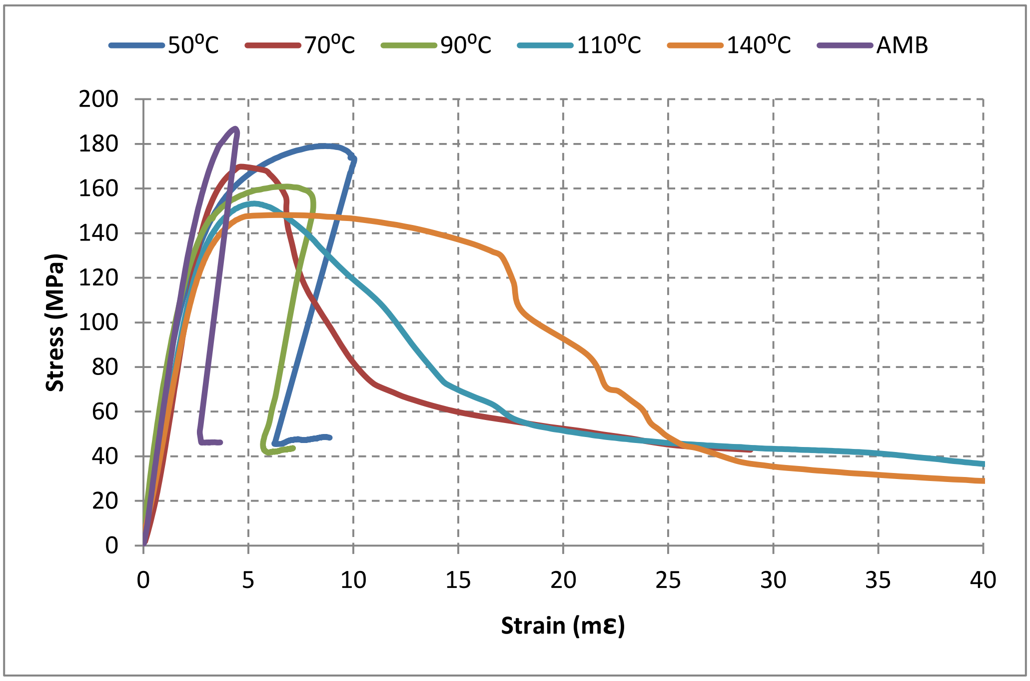

Figure A3 13: Chromitite tested at 10 MPa confinement, different temperatures

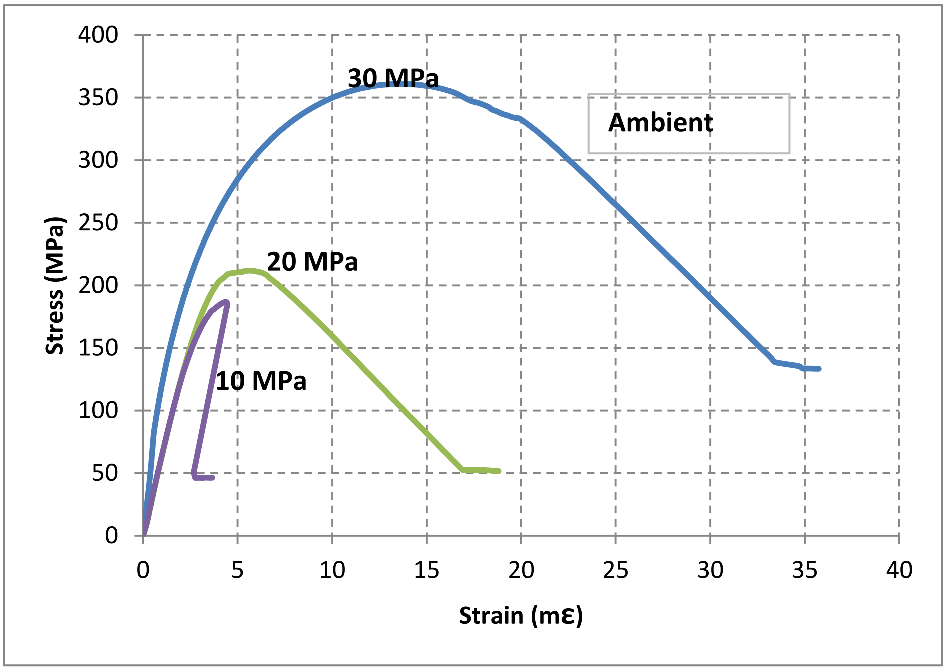

Figure A3 14: Chromitite tested at ambient temperature, different confinements

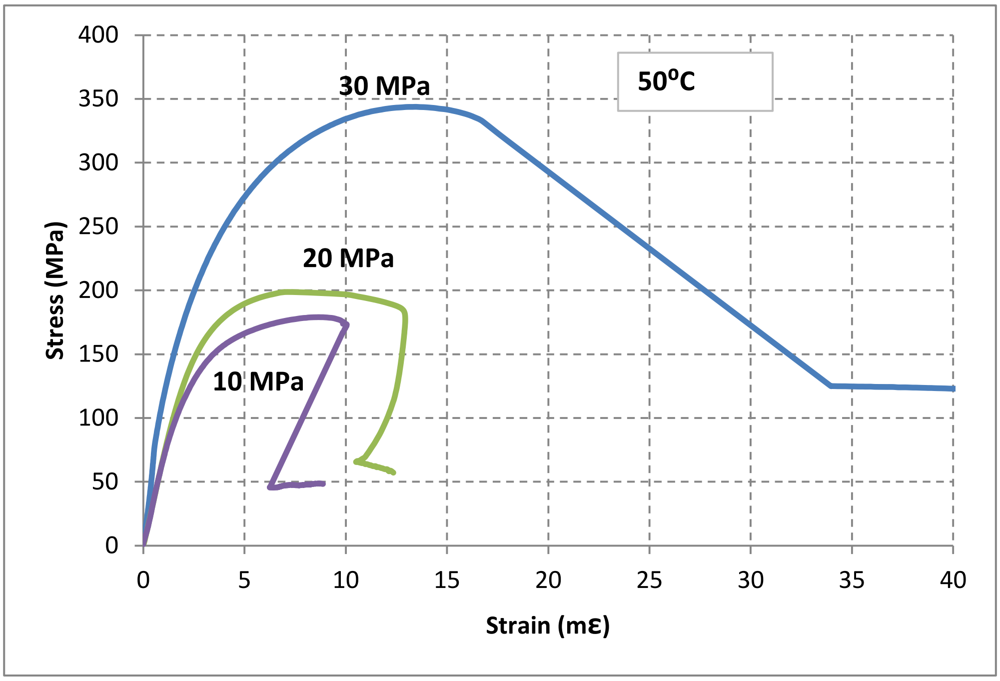

Figure A3 15: Chromitite tested at 50°C, different confinements

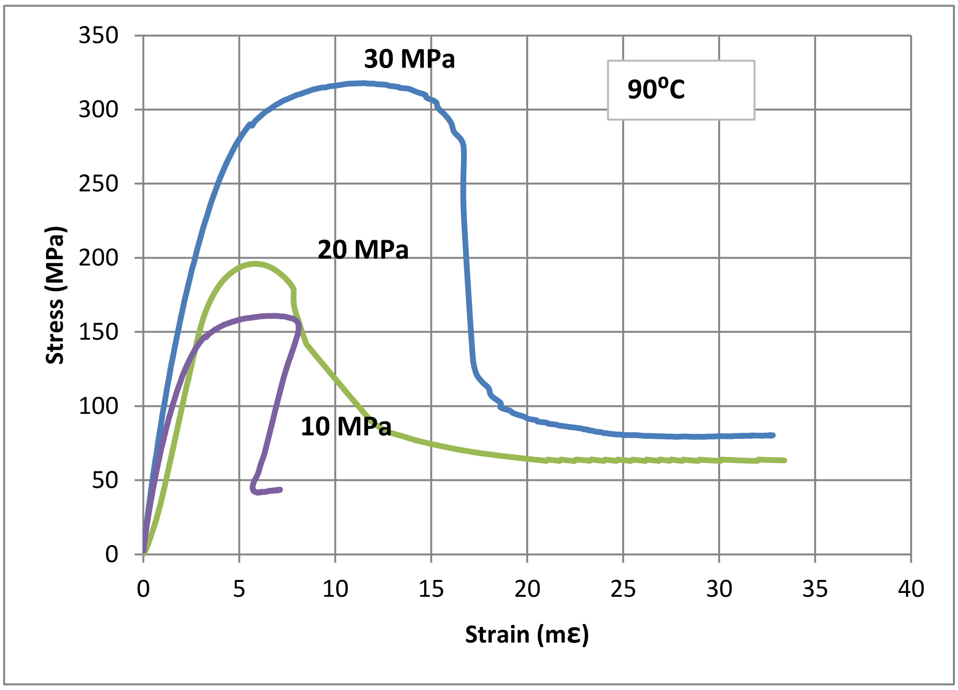

Figure A3 16: Chromitite tested at 90°C, different confinements

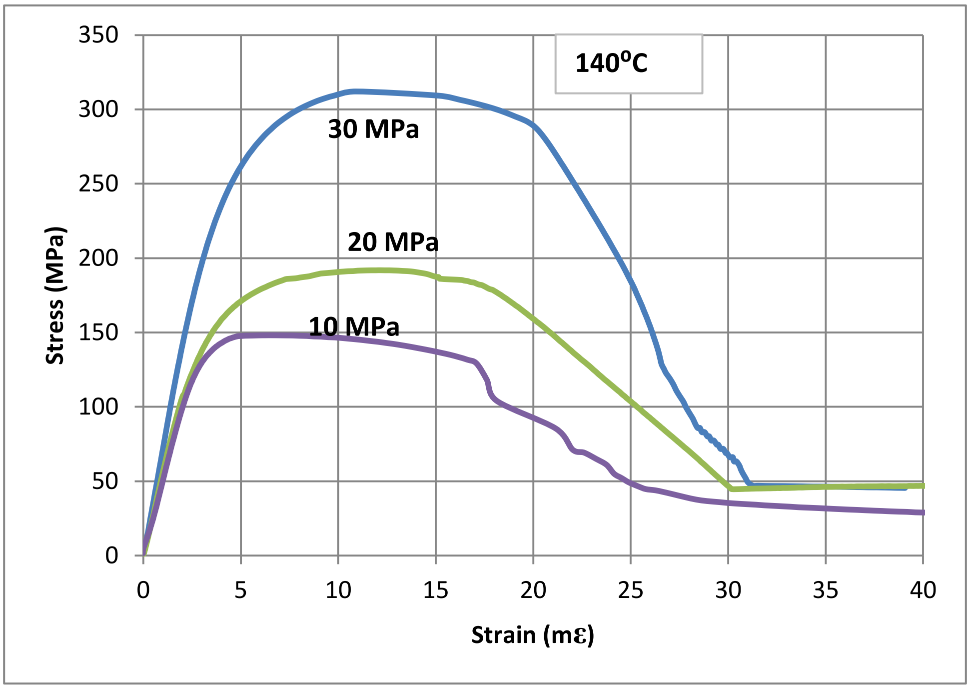

Figure A3 17: Chromitite tested at 140°C, different confinements

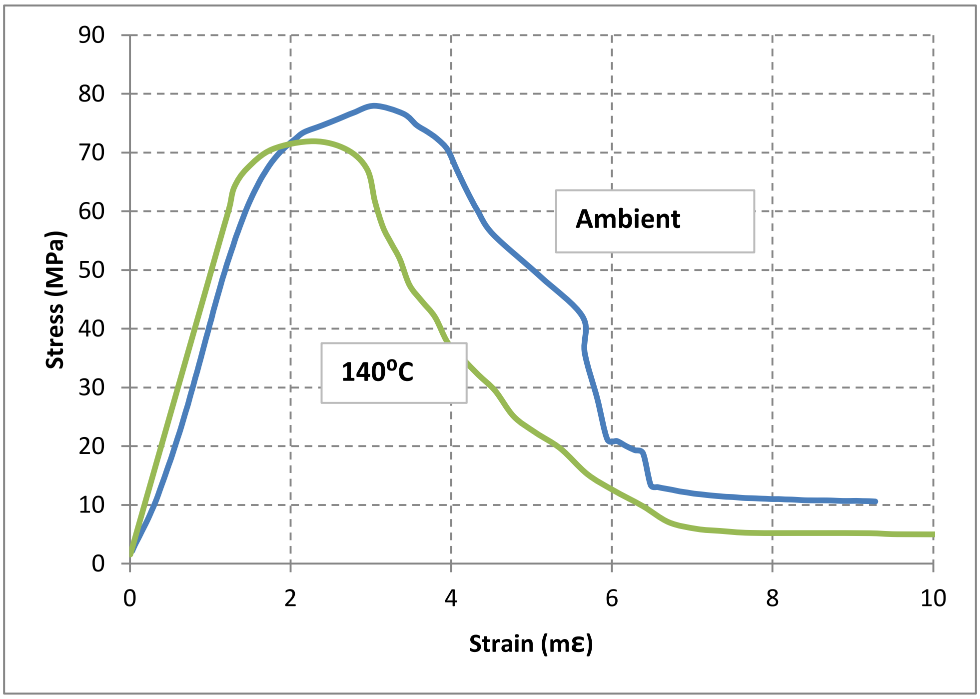

Figure A3 18: Chromitite tested at ambient and 140°C, zero confinement

Table A3 3: Young’s modulus and Poisson's Ratio of chromitite

	AMB	50°C	70°C	90°C	110°C	140°C
			Young’s modulus (GPa)			
0 MPa	49.7					47.9
10 MPa	58.5	56.2	55.3	53.8	52.2	51.7
20 MPa	60.5	58.2		57.9		55.3
30 MPa	64.9	63.1		61.6		59.7
			Poisson’s Ratio			
0 MPa	0.42					0.43
10 MPa	0.42	0.43	0.43	0.42	0.43	0.44
20 MPa	0.43	0.42		0.42		0.43
30 MPa	0.44	0.42		0.42		0.43

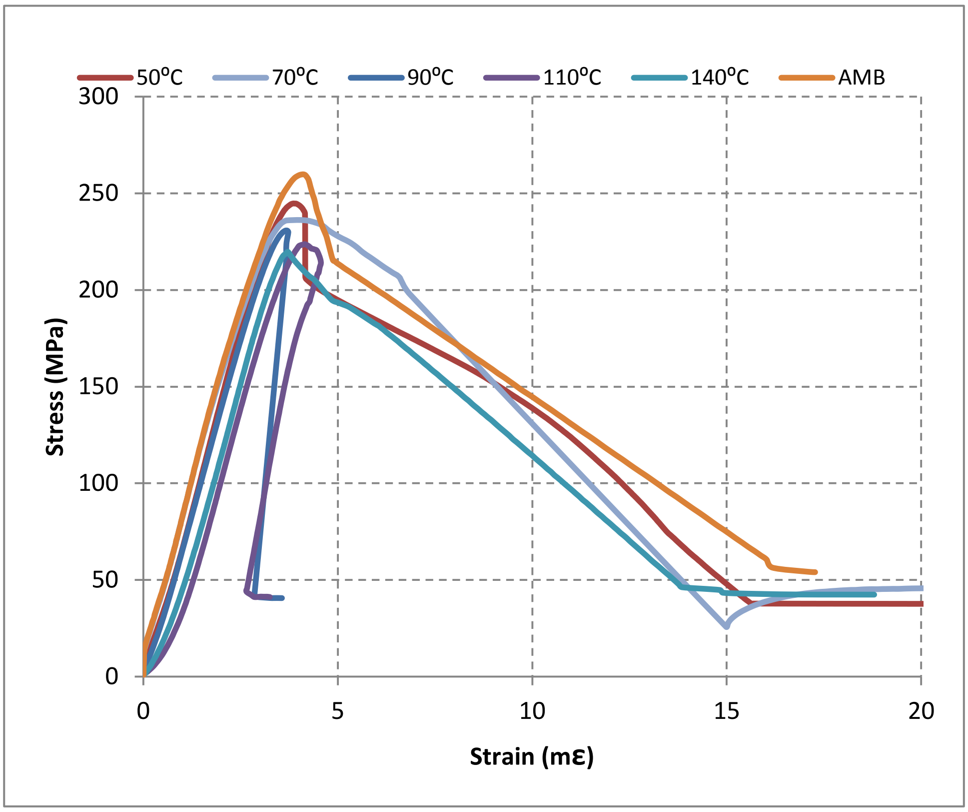

Figure A3 19: Leuconorite tested at 10 MPa confinement, different temperatures

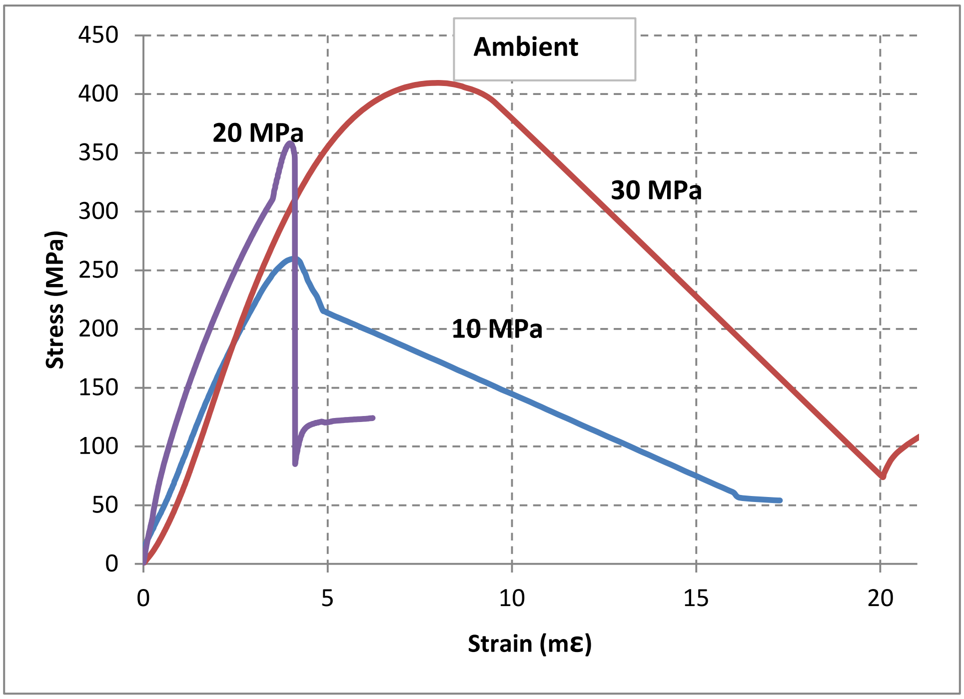

Figure A3 20: Leuconorite tested at ambient temperature, different confinements

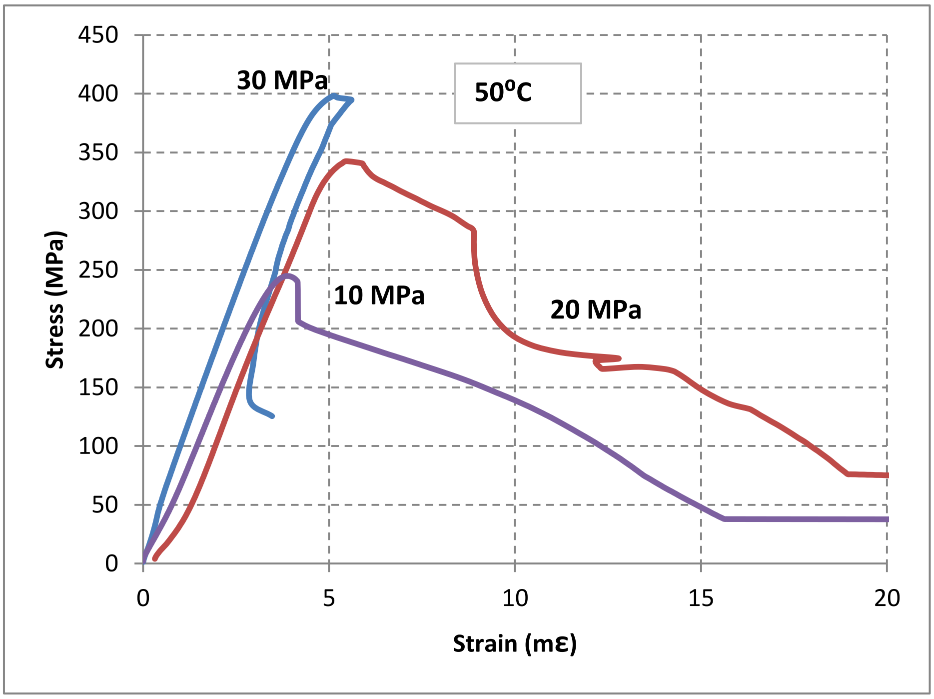

Figure A3 21: Leuconorite tested at 50°C, different confinements

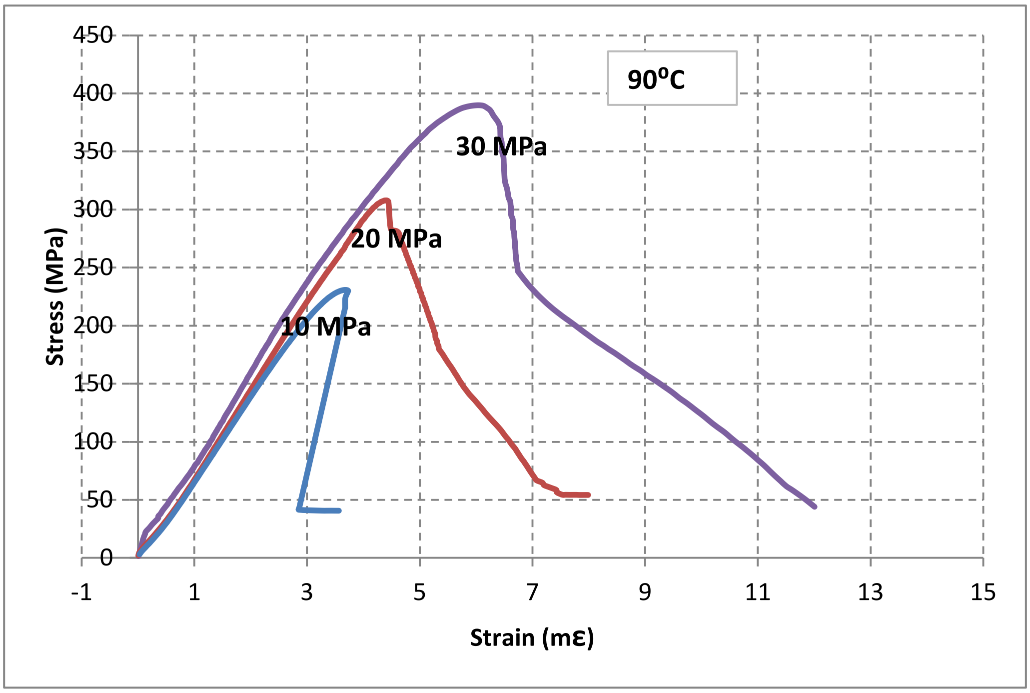

Figure A3 22: Leuconorite tested at 90°C, different confinements

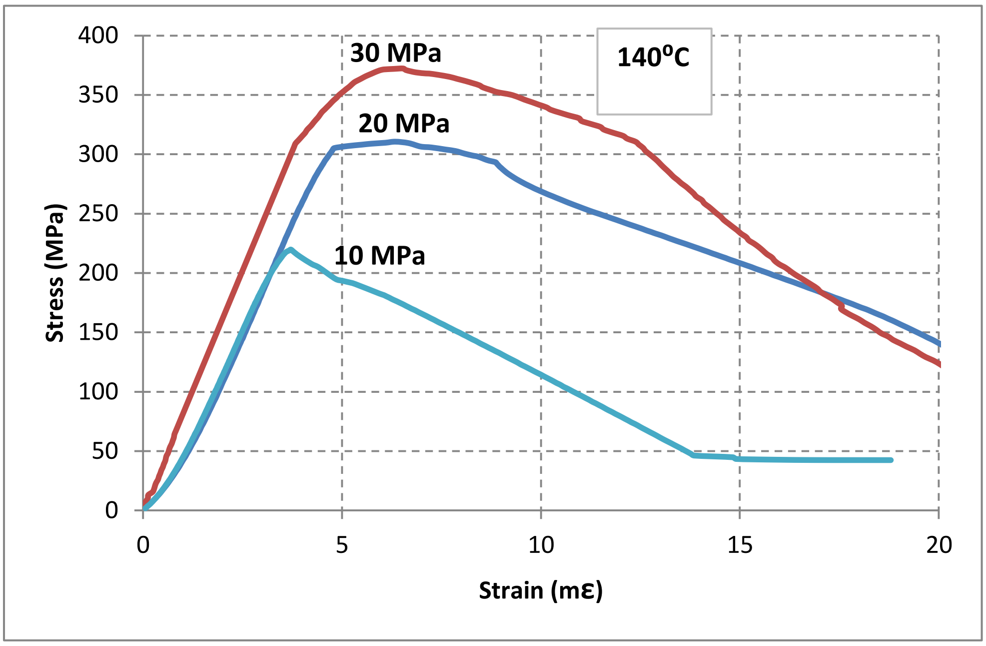

Figure A3 23: Leuconorite tested at 140°C, different confinements

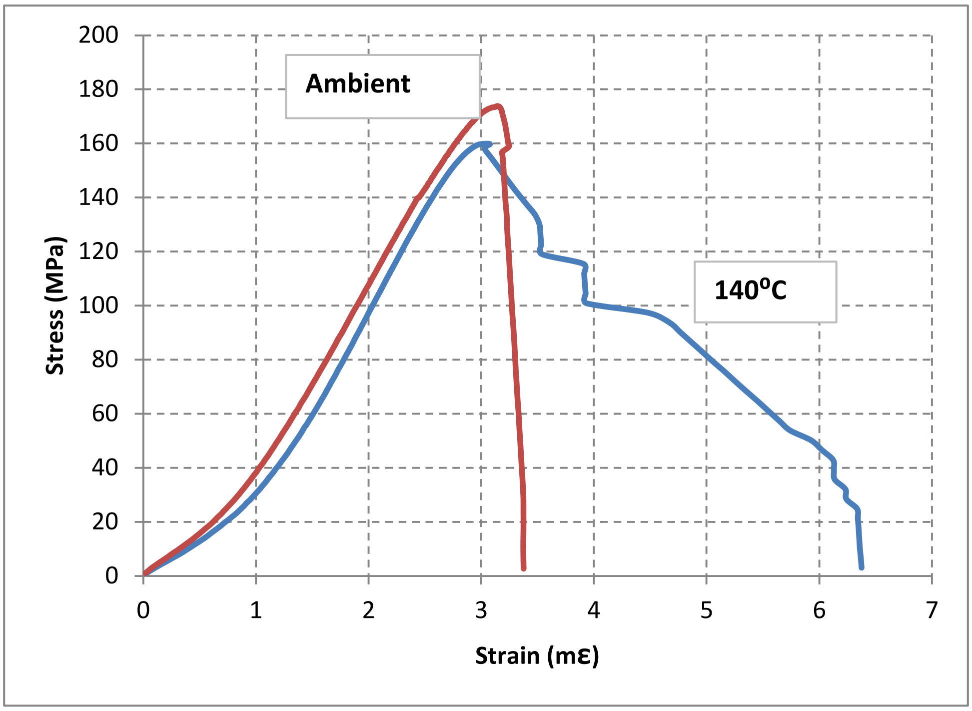

Figure A3 24: Leuconorite tested at ambient and 140°C, zero confinement

Table A3 4: Young's modulus and Poisson's Ratio of leuconorite

	AMB	50°C	70°C	90°C	110°C	140°C
			Young's modulus (GPa)			
0 MPa	75.0					72.0
10 MPa	78.4	76.6	74.1	73.5	72.2	70.7
20 MPa	81.9	80.4		77.4		76.3
30 MPa	87.1	83.8		79.9		80.0
			Poisson's Ratio			
0 MPa	0.33					0.34
10 MPa	0.34	0.34	0.34	0.34	0.33	0.33
20 MPa	0.33	0.34		0.33		0.33
30 MPa	0.33	0.34		0.34		0.33

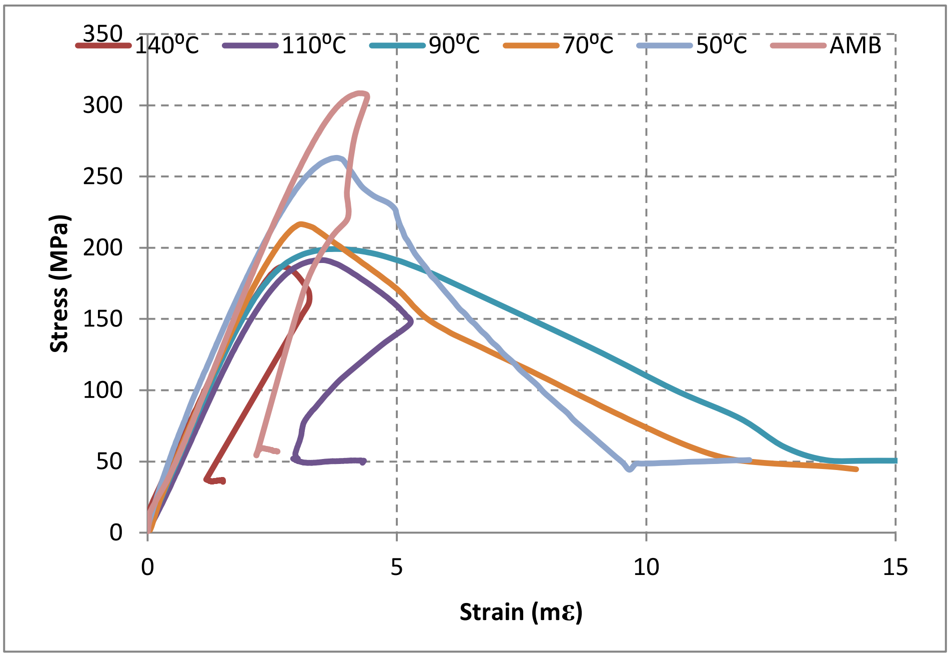

Figure A3 25: Vari-textured anorthosite tested at 10 MPa confinement, different temperatures

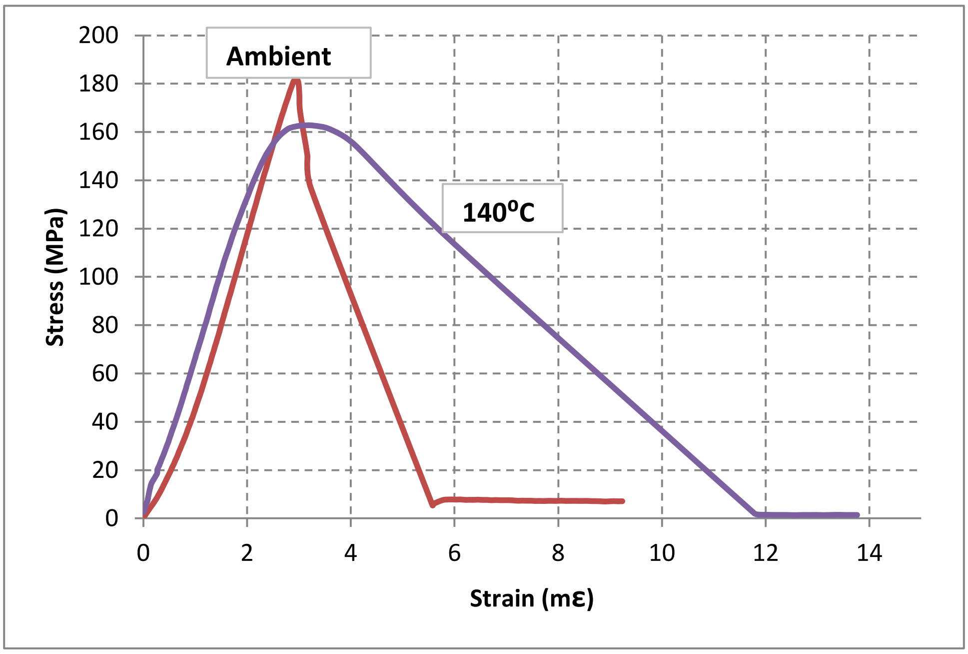

Figure A3 25: Vari-textured anorthosite tested at ambient and 140°C, zero confinement

Table A3 5: Young’s modulus and Poisson's Ratio of vari-textured anorthosite

	AMB	50°C	70°C	90°C	110°C	140°C
			Young’s modulus (GPa)			
0 MPa	73.48					71.5
10 MPa	83.65	81.27	78.98	76.21	74.63	72.09
			Poisson’s Ratio			
0 MPa	0.37					0.37
10 MPa	0.37	0.38	0.37	0.37	0.37	0.37

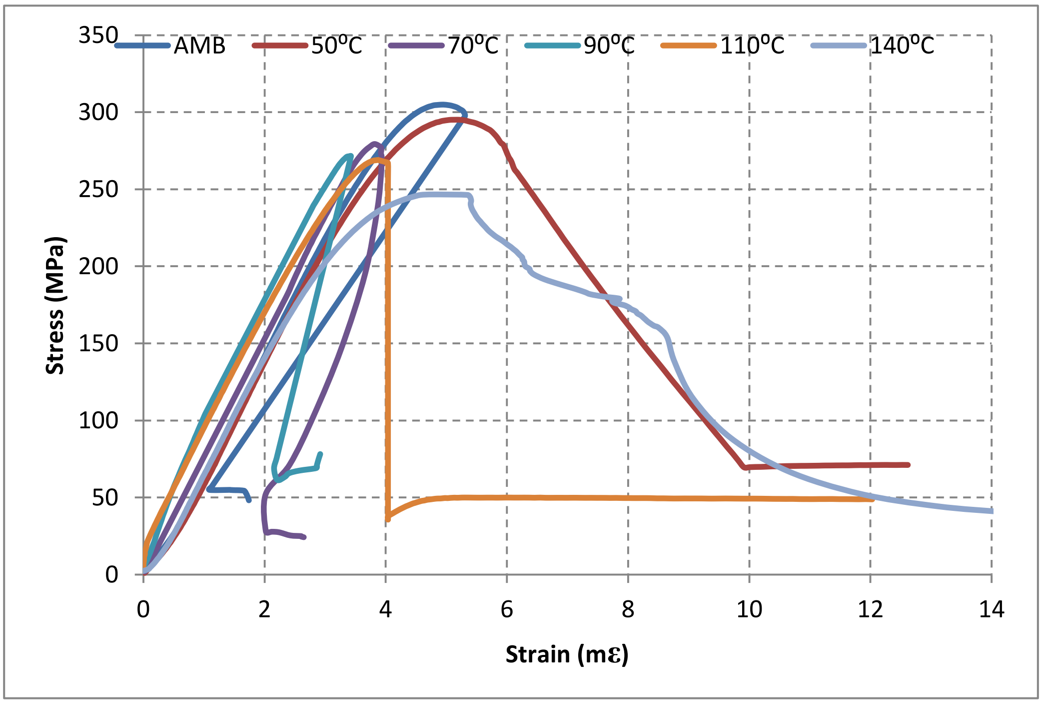

Figure A3 26: Anorthosite-chromitite tested at 10 MPa confinement, different temperatures

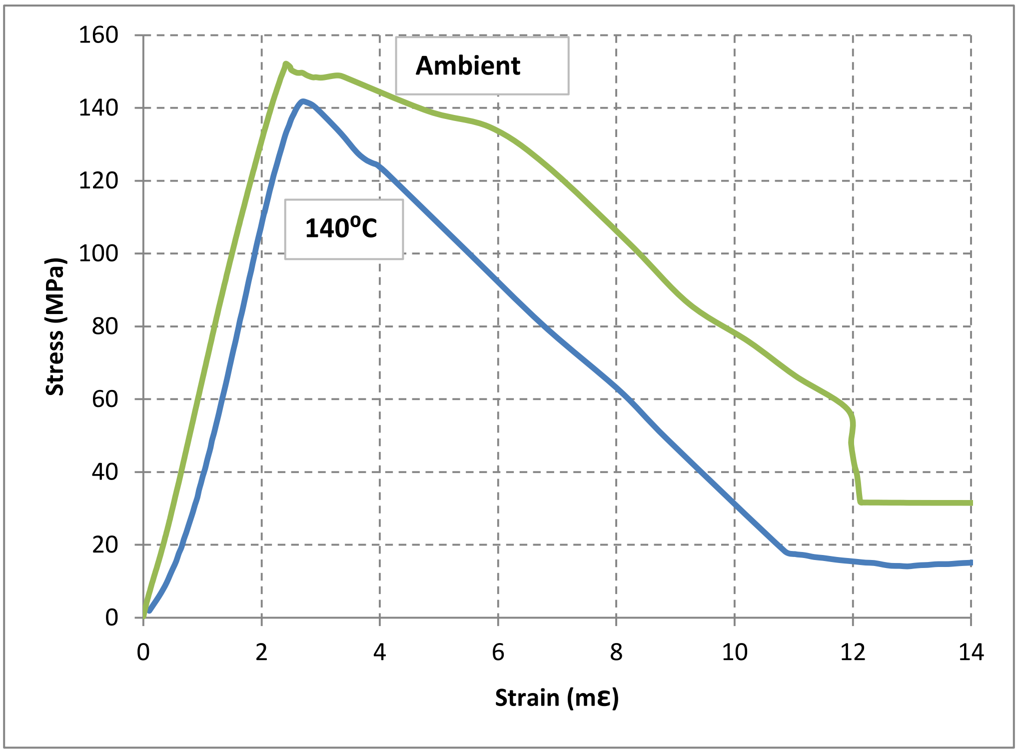

Figure A3 27: Anorthosite-chromitite tested at ambient and 140°C, zero confinement

Table A3 6: Young's modulus and Poisson's Ratio of anorthosite chromitite

	AMB	50°C	70°C	90°C	110°C	140°C
			Young's modulus (GPa)			
0 MPa	70.5					67.6
10 MPa	80.6	78.3	77.8	75.9	74.5	72.3
			Poisson's Ratio			
0 MPa	0.40					0.39
10 MPa	0.39	0.39	0.39	0.38	0.40	0.40

APPENDIX A4

Detailed procedure of using Video Extensometer for the measurement of longitudinal and transversal thermal strain

After placement of the specimen in the oven and the illumination of the oven, the set up of the video extensometer for data capturing follows. The steps involved are presented as follow:

a) Test setting is done by selecting the type of strain to be measured (true or nominal), name of specimen, number and colour of the markers as shown in Figure A4 1(a)
b) This is followed by image optimization, which is the adjustment of brightness and contrast in order to have good image (Figure A4 1(b))
c) The next step is to search for markers. The markers can only be visible if there is a sharp colour contrast between the specimen and the marker in the presence of appropriate illumination. That is why white markers were used for specimens with dark-coloured minerals, while black markers were used for specimens with light-coloured minerals (Figure A4 2 (a)).
d) Scale calibration is next. Here, the centre to centre measurement (real length, measured in mm) of the markers is fed into software as a reference for further measurements (Figure A4 2 (b)).
e) The last step is initialization, which marks the beginning of the test (Figure A4 2 (c) and (d)).

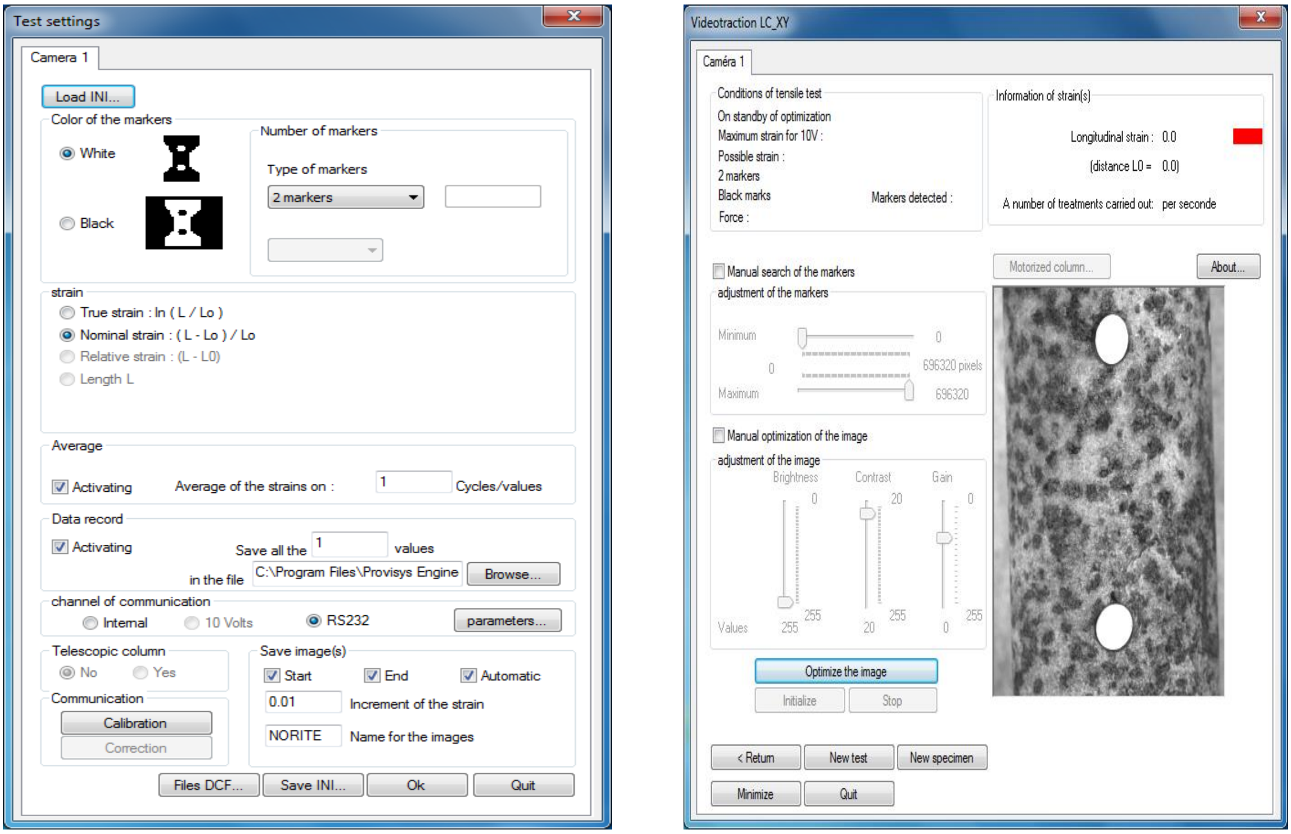

(a) (b)

Figure A4 1 (a) Test setting and (b): and image optimization.

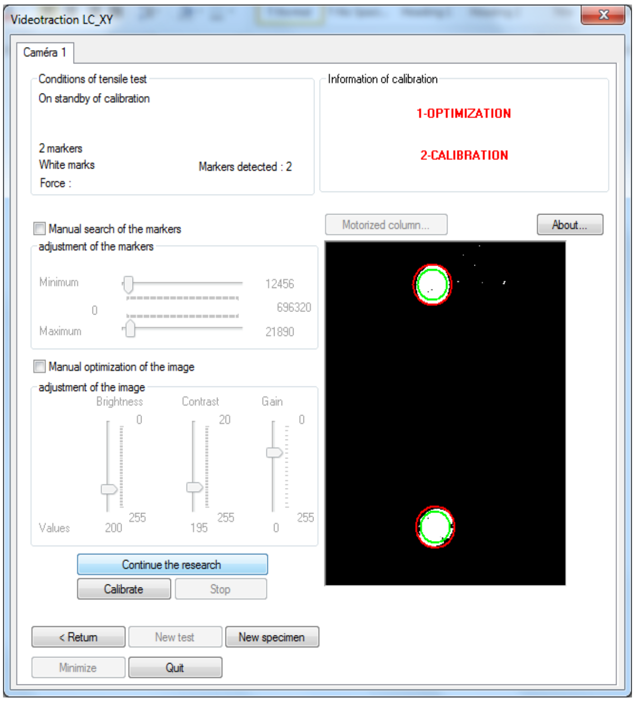

(a)

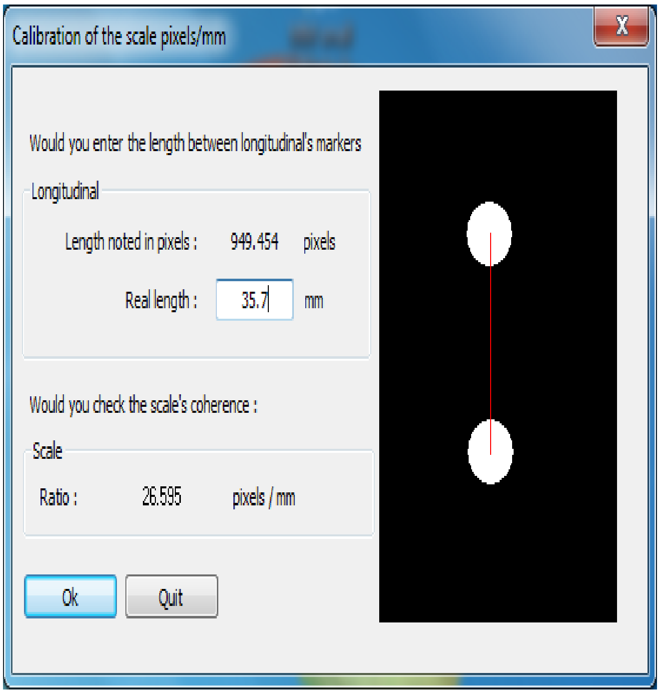

(b)

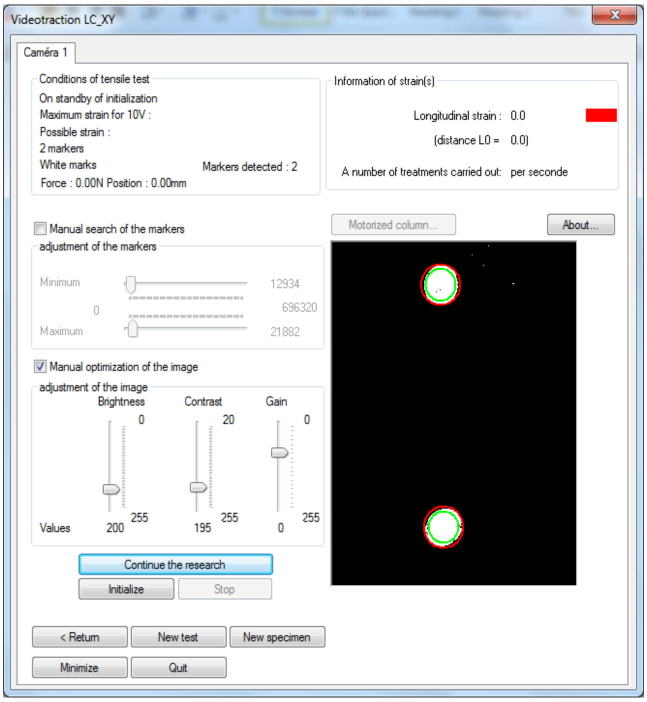

(c)

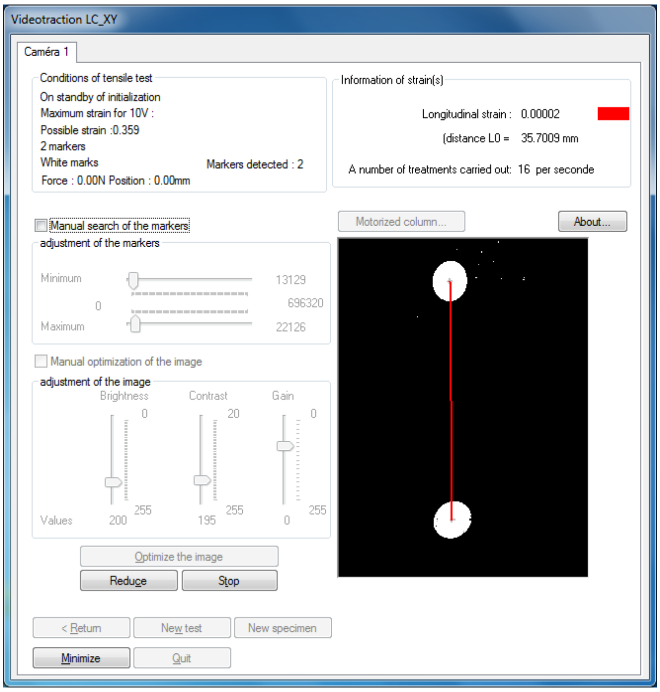

(d)

Figure A4 2 (a)-(d): Optimization/calibration, search for markers and initialization of test.

The same procedure as described above is also used for the measurement of transverse strain except that additional two markers were added horizontally to the specimen as shown in Figure A4 3.

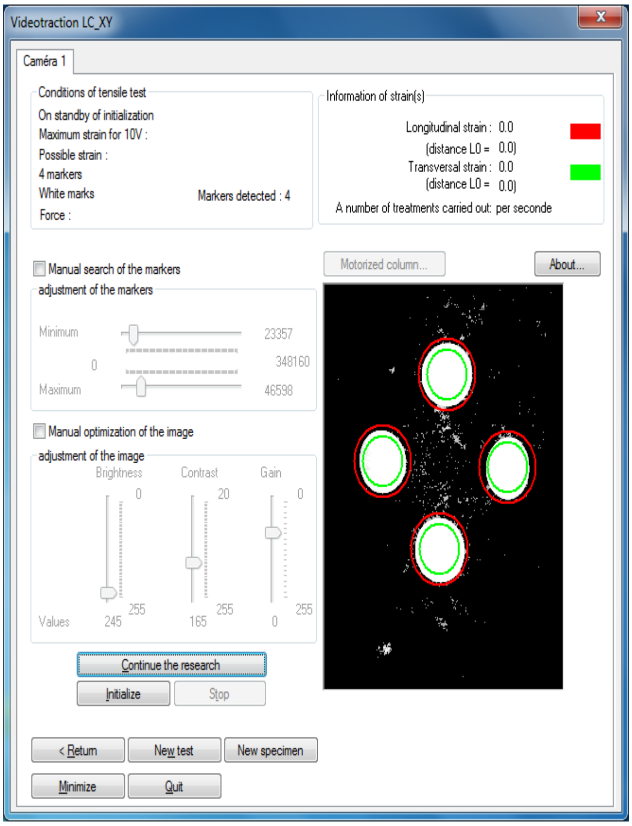

Figure A4 3: Specimen with four markers.

APPENDIX A5

Detailed procedure employed in the measurement of unconfined coefficient of thermal expansion.

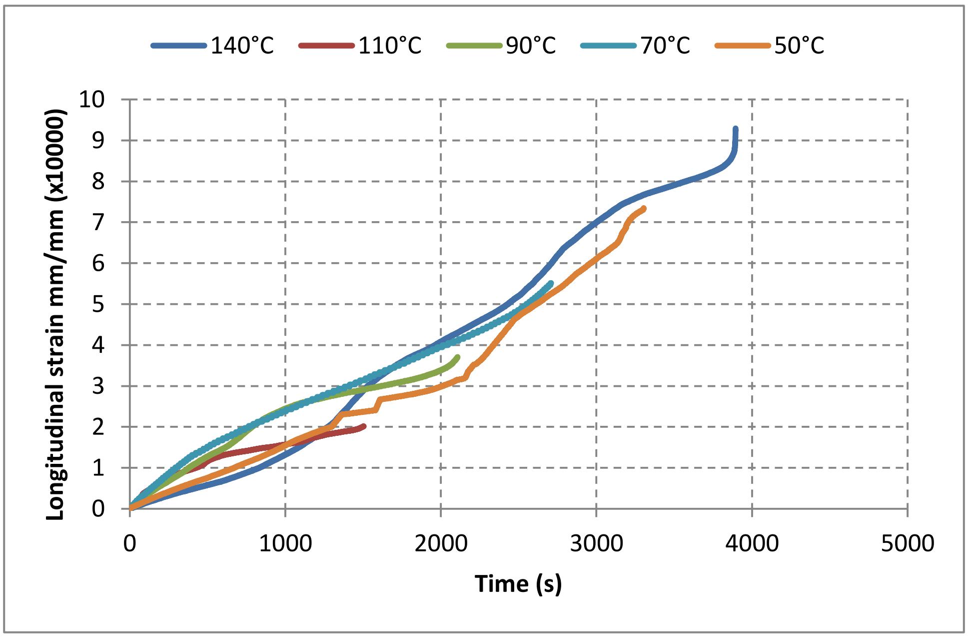

Figure A5 1: The plot of longitudinal strain against time for leuconorite at different temperatures

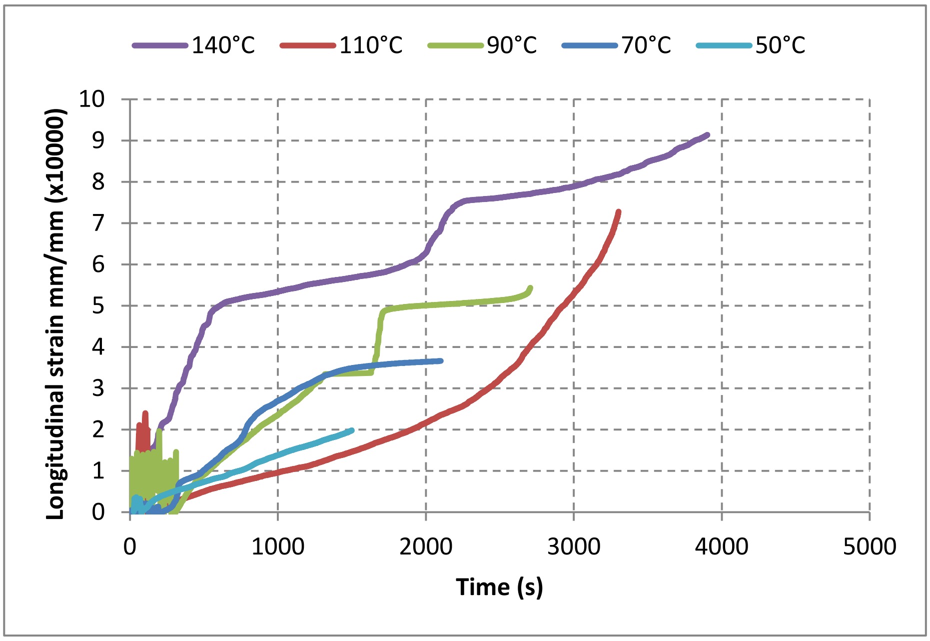

Figure A5 2: Longitudinal strain against time for chromitite at different temperatures

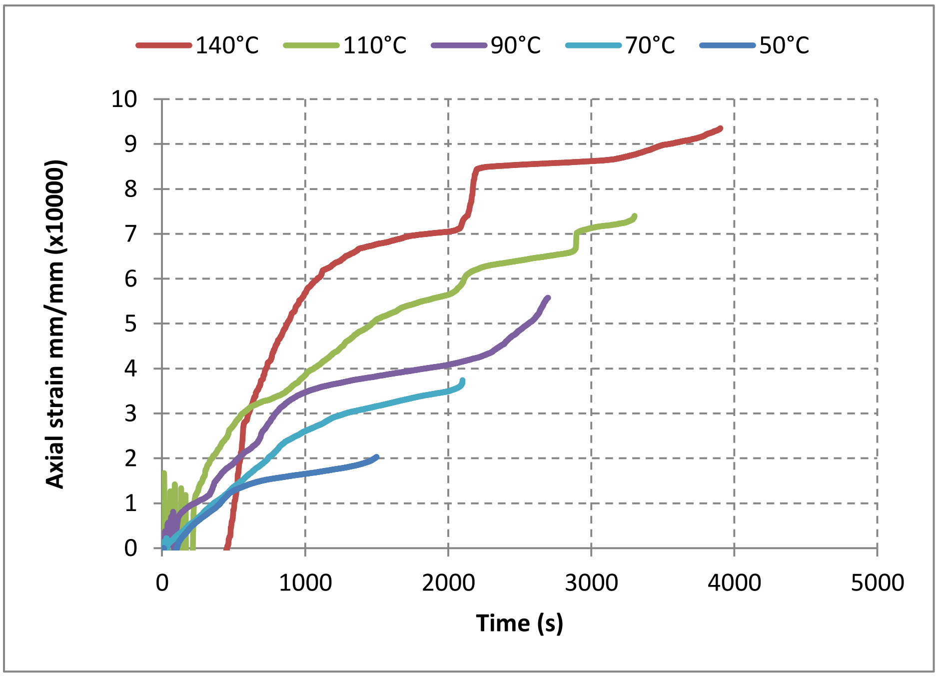

Figure A5 3: Longitudinal strain against time for mottled anorthosite at different temperatures

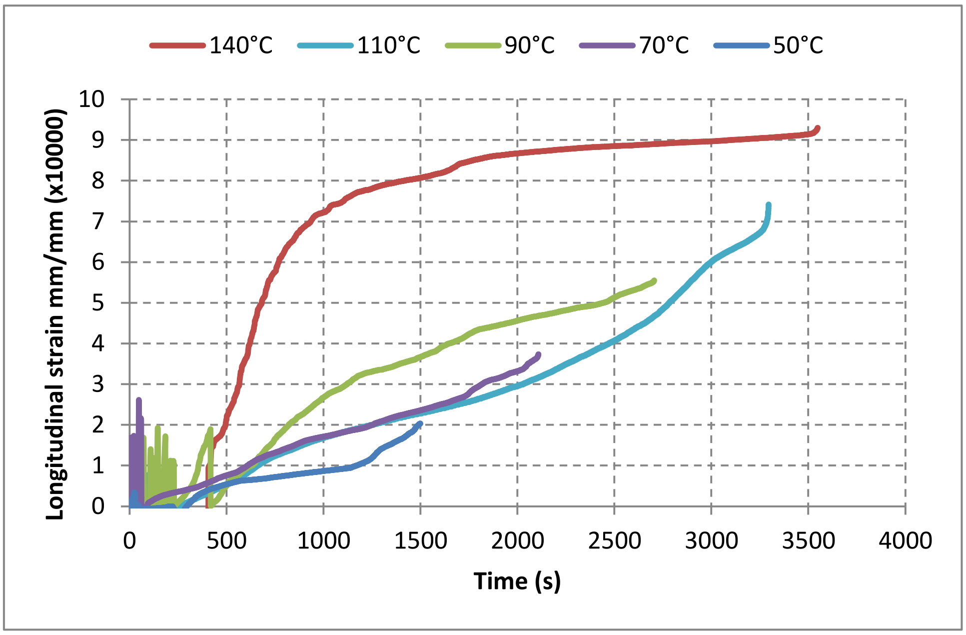

Figure A5 4: Longitudinal strain against time for pyroxenite at different temperatures

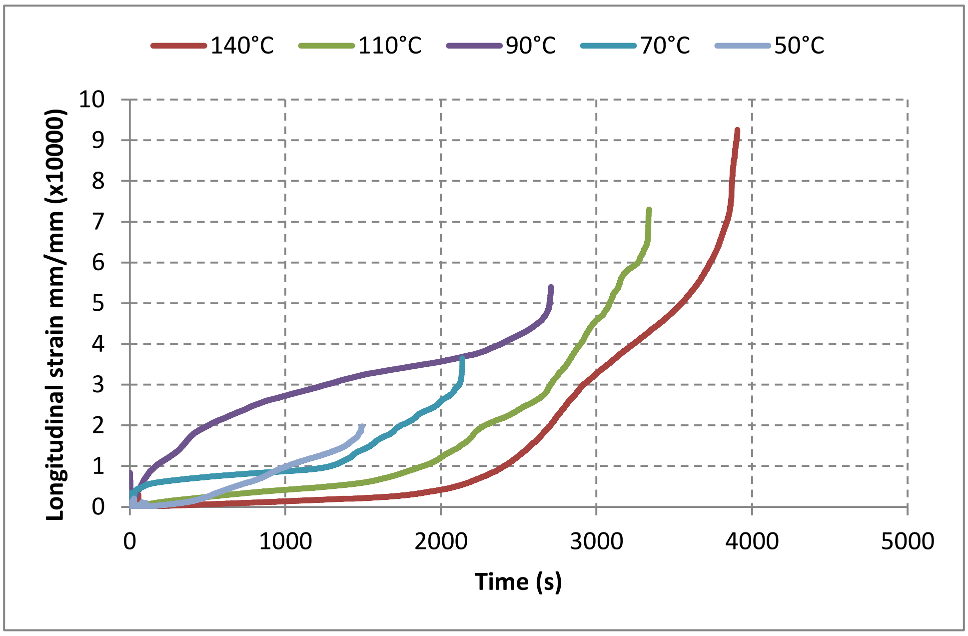

Figure A5 5: Longitudinal strain against time for granite at different temperatures

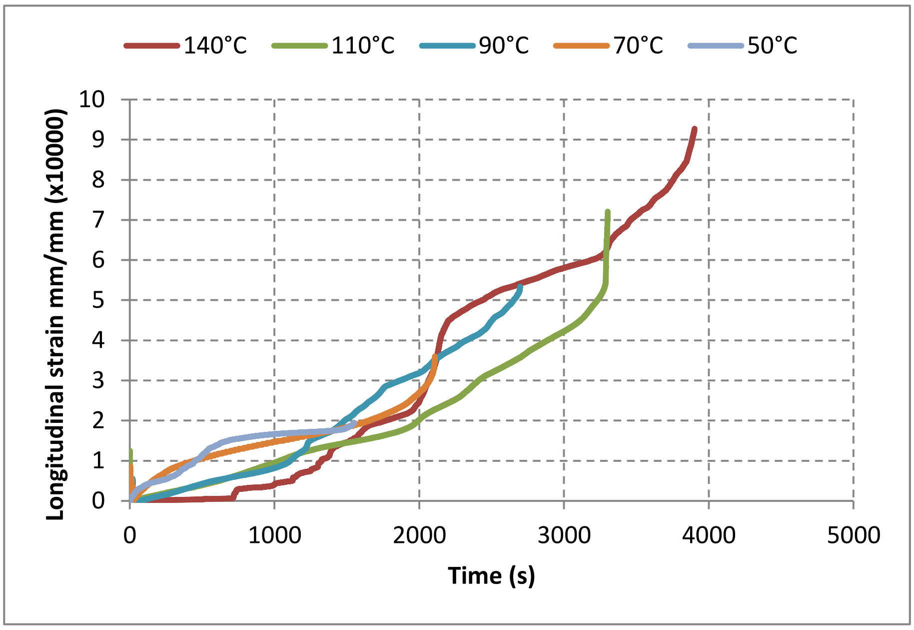

Figure A5 6: Longitudinal strain against time for granite at different temperatures

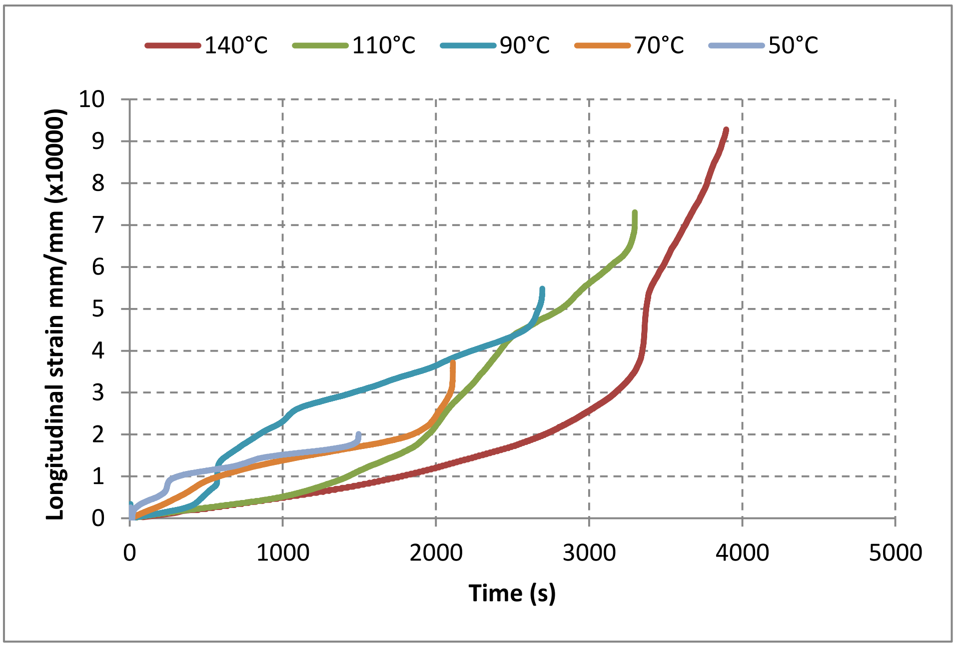

Figure A5 7: Longitudinal strain against time for granofels at different temperatures

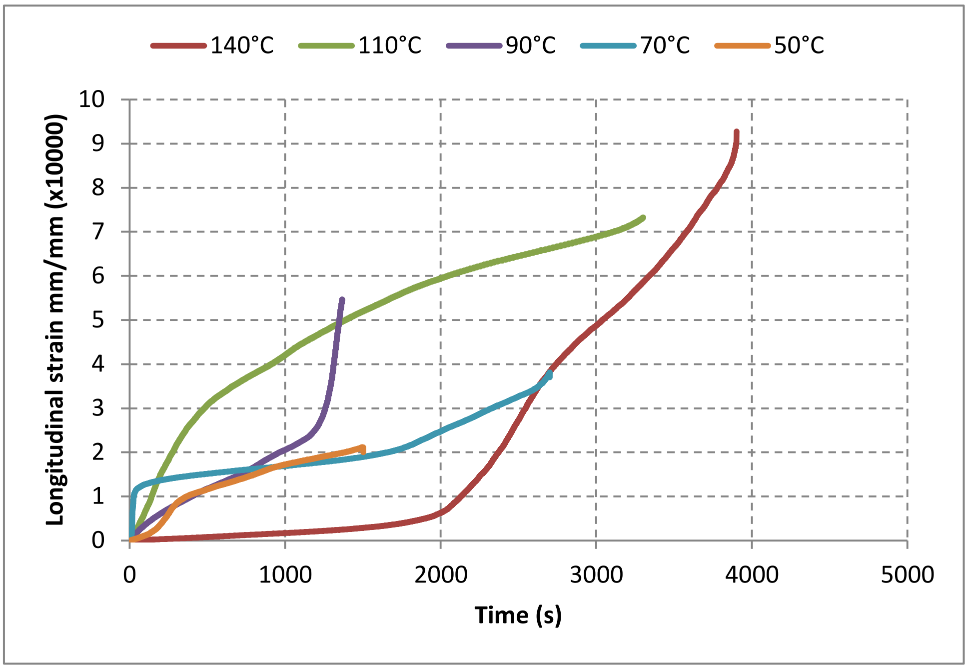

Figure A5 8: Longitudinal strain against time for vari-textured anorthosite at different temperatures

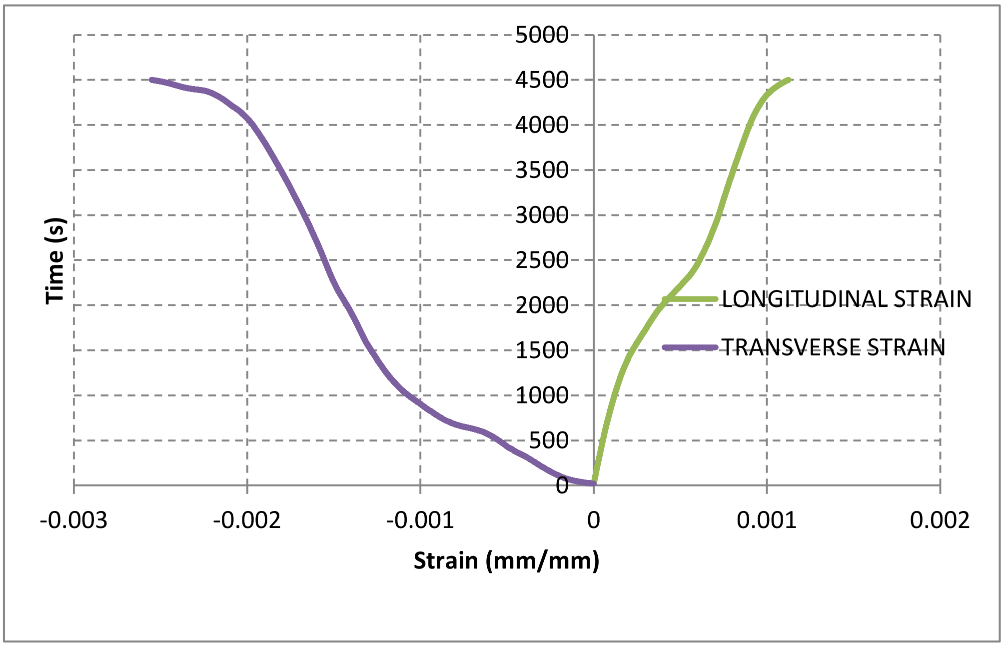

Figure A5 9: Longitudinal and transversal strain against time for chromitite at 140°C

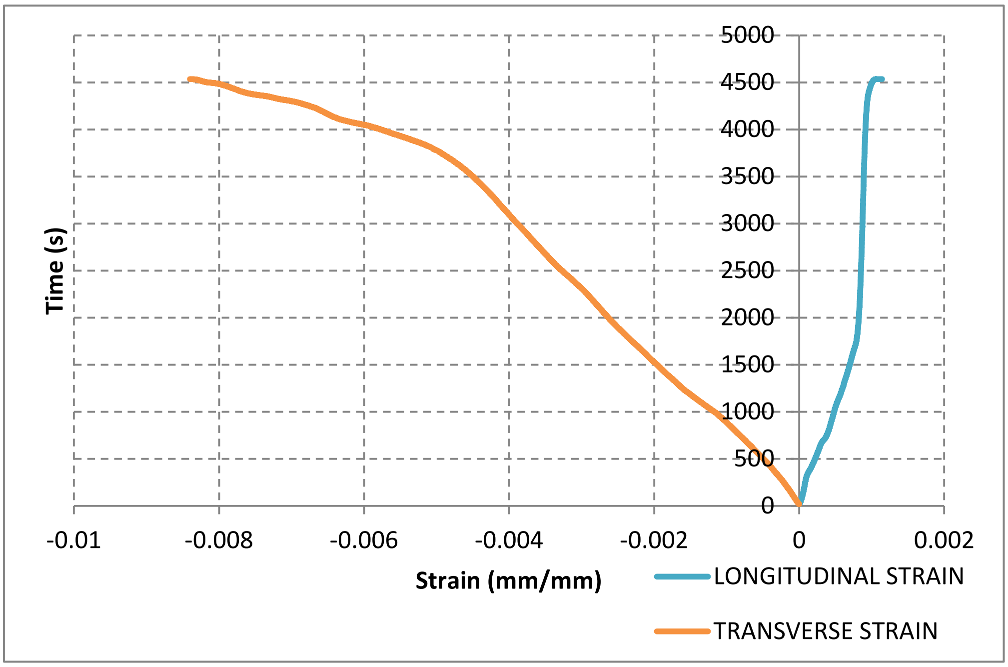

Figure A5 10: Longitudinal and transversal strain against time for mottled anorthosite at 140°C

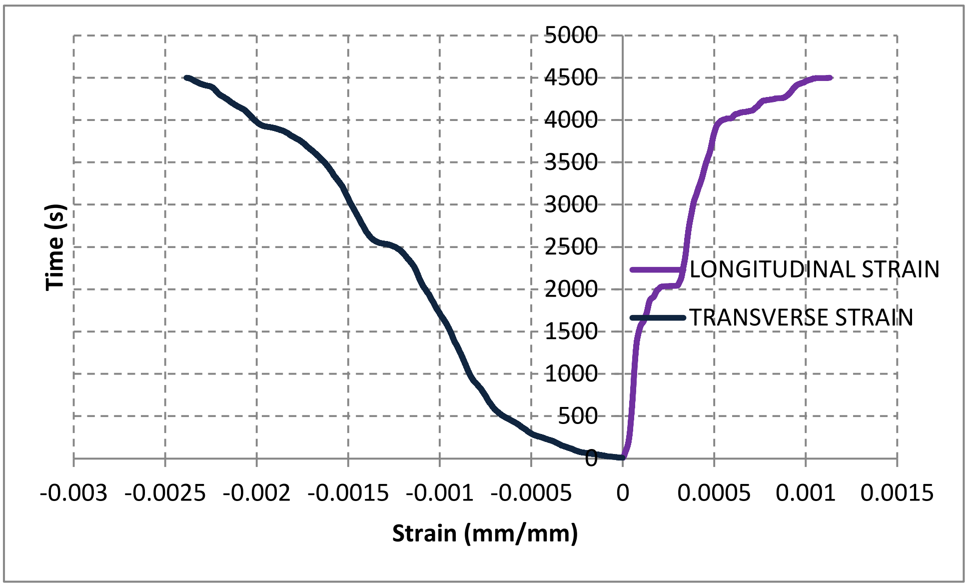

Figure A5 11: Longitudinal and transversal strain against time for leuconorite at 140°C

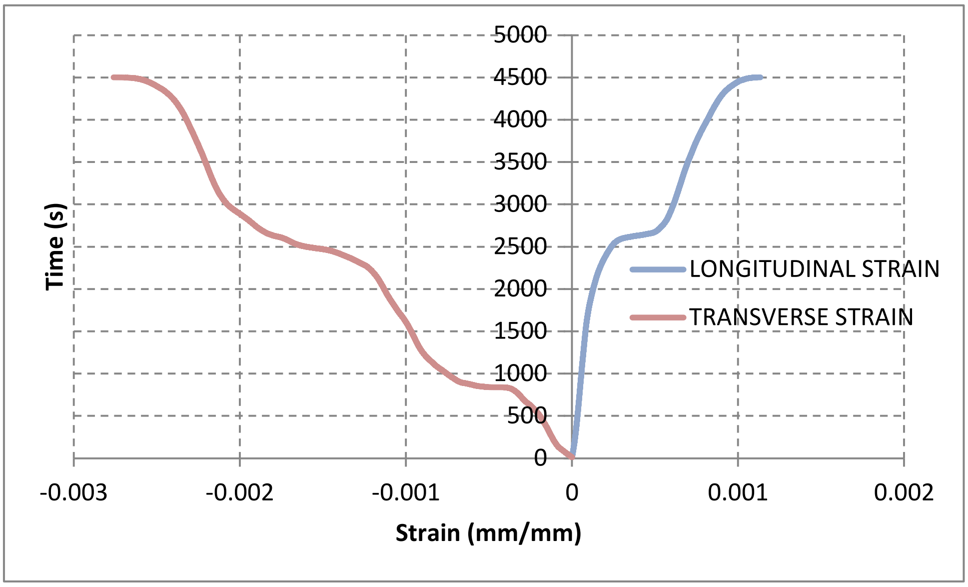

Figure A5 12: Longitudinal and transversal strain against time for granofel at 140°C

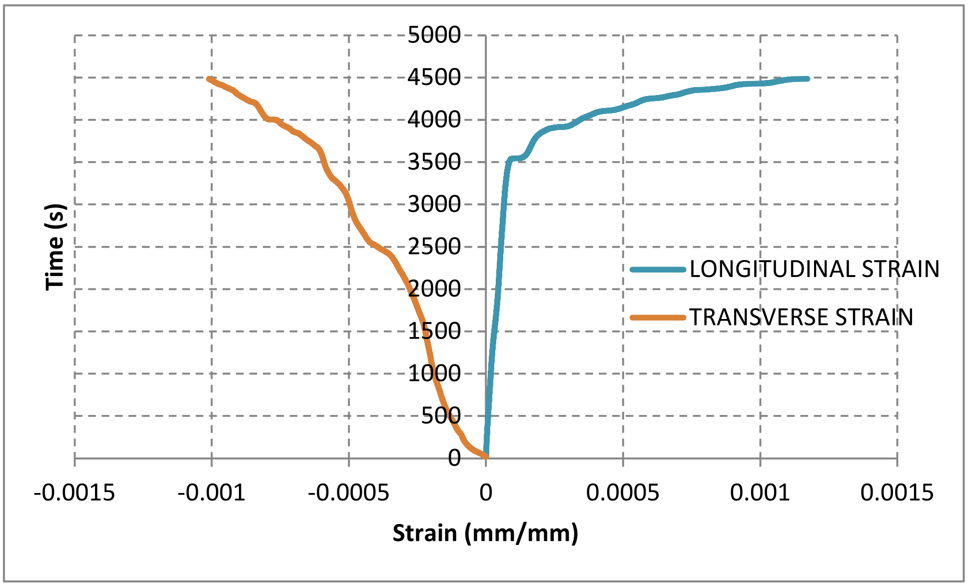

Figure A5 13: Longitudinal and transversal strain against time for gabbronorite at 140°C

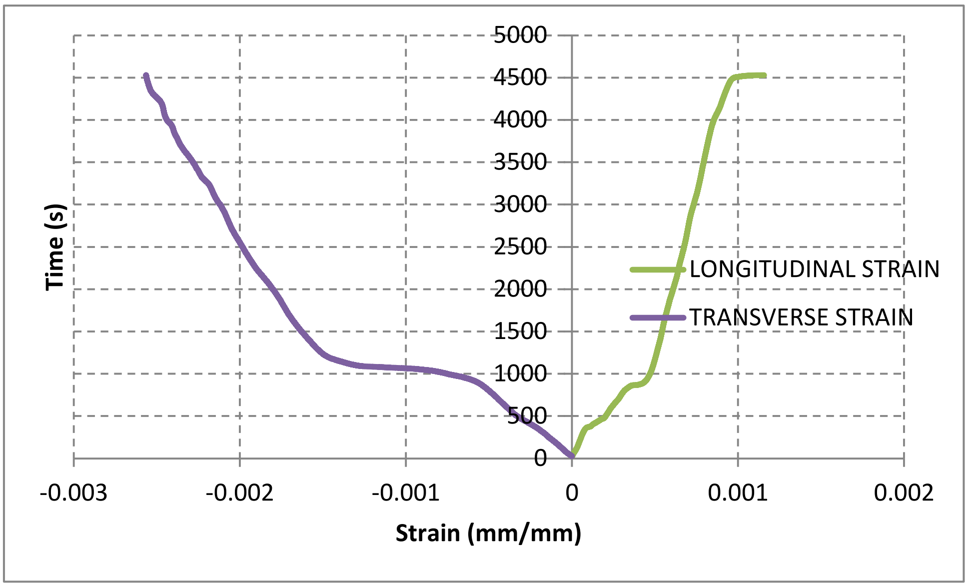

Figure A5 14: The plot of longitudinal and transversal strain against time for granite at 140°C

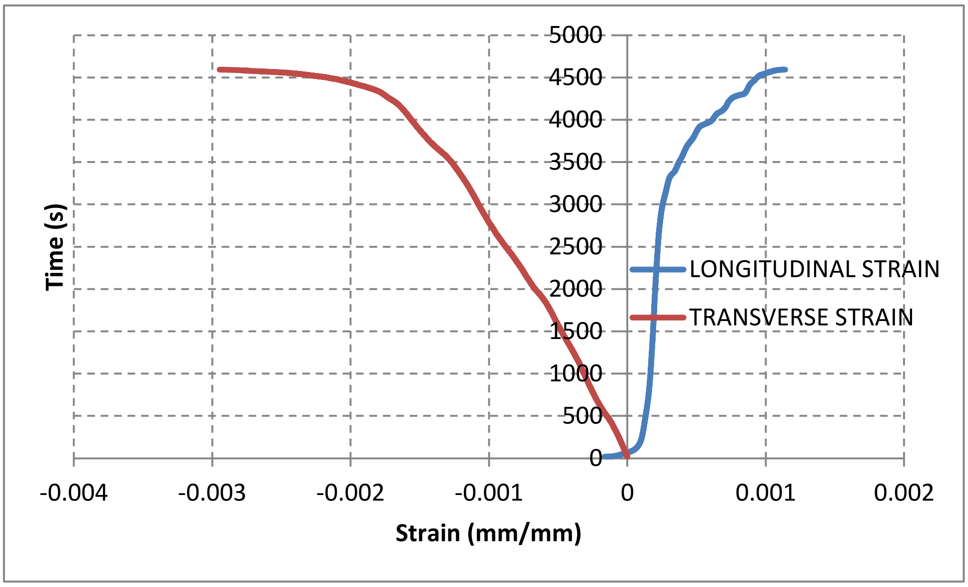

Figure A5 15: Longitudinal and transversal strain against time for vari-texture anorthosite at 140°C

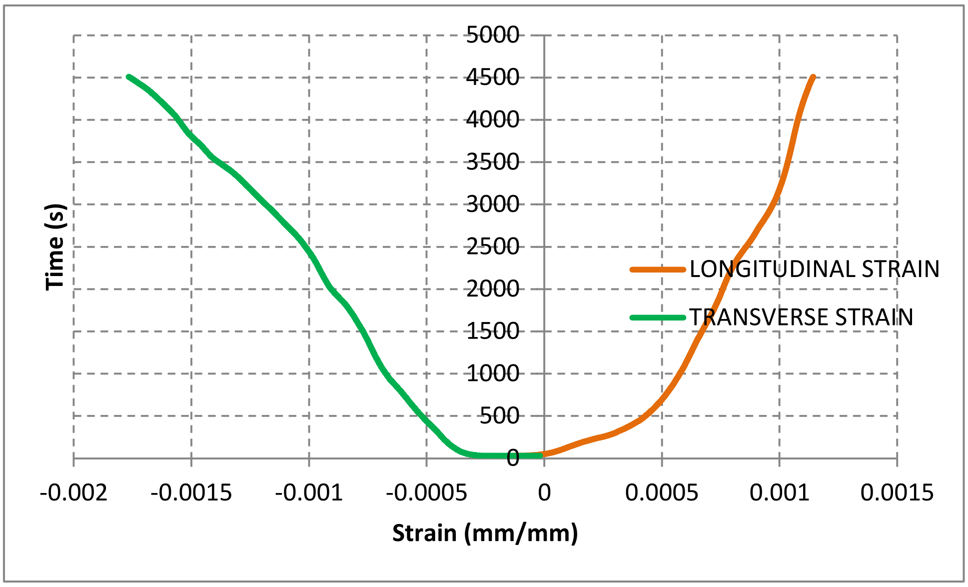

Figure A5 16: Longitudinal and transversal strain against time for norite at 140°C

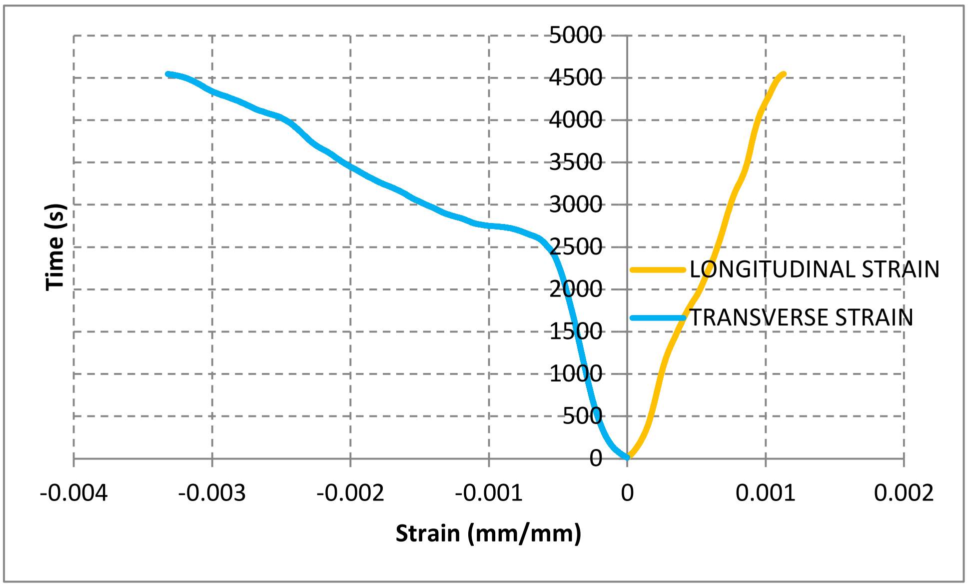

Figure A5 17: Longitudinal and transversal strain against time for pyroxenite at 140°C

APPENDIX A6

The plots of pre-peak, peak and residual dilation angles.

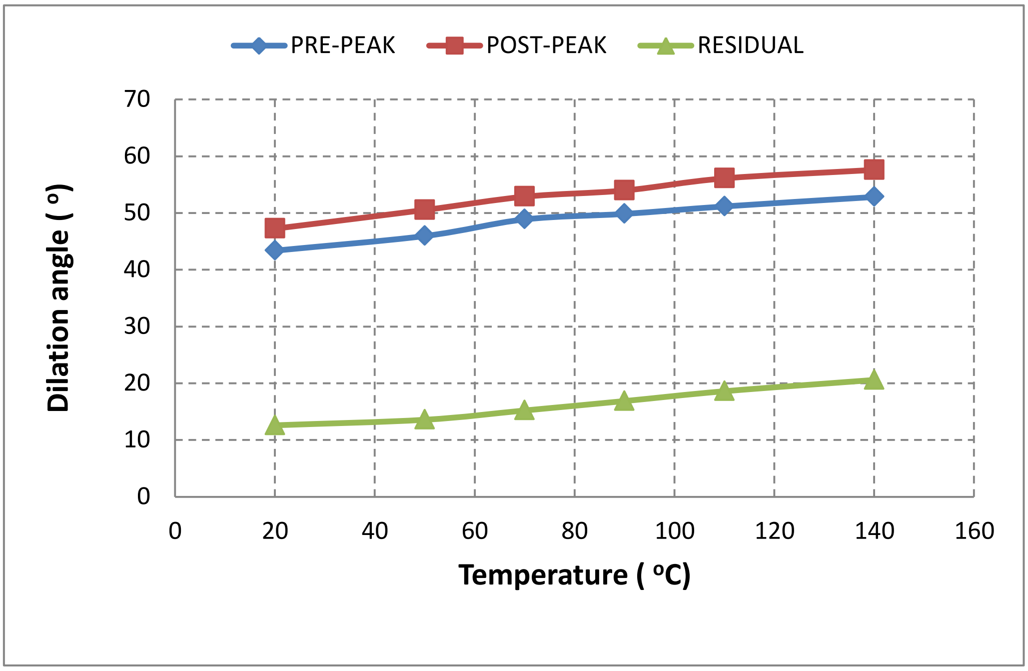

Figure A6 1: Dilation angle against temperature for pyroxenite.

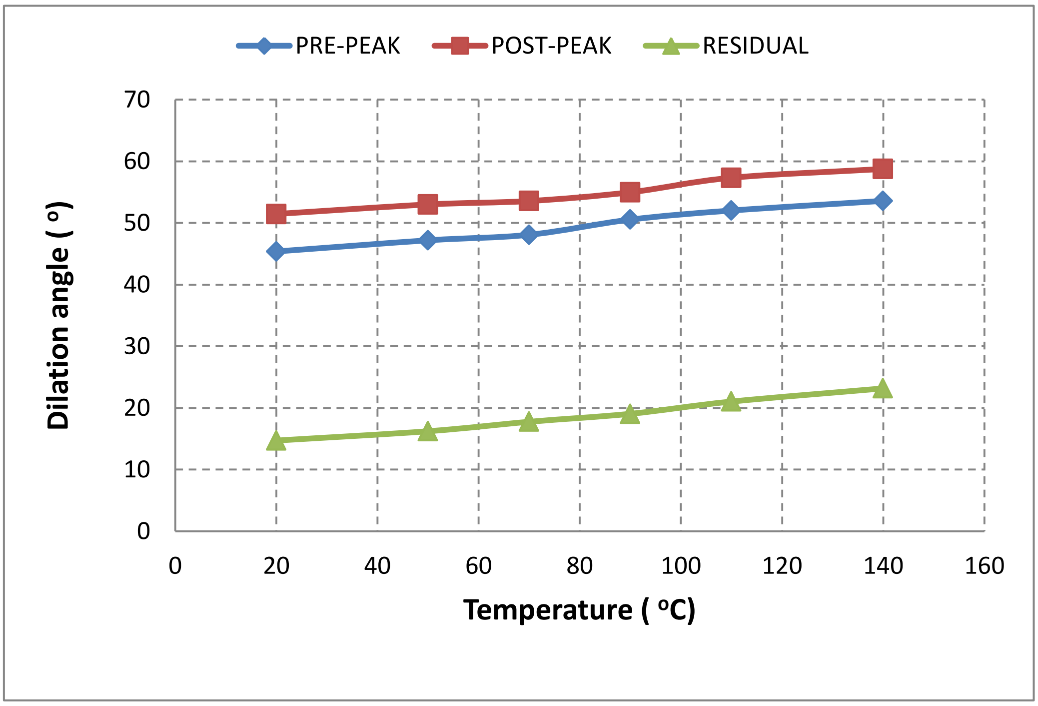

Figure A6 2: Dilation angle against temperature for mottled anorthosite.

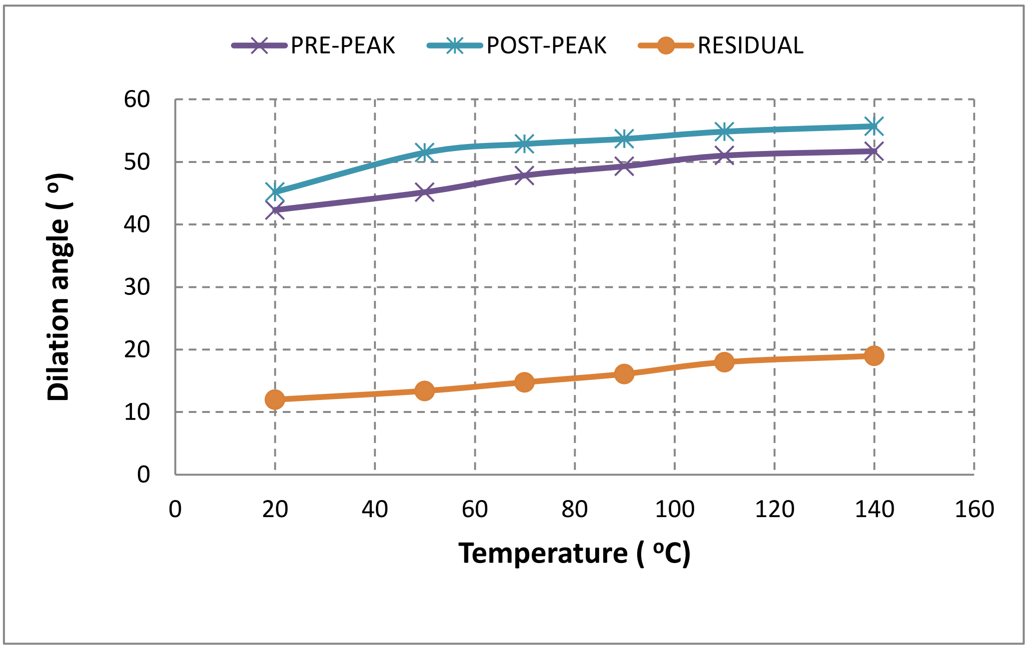

Figure A6 3: Plot of dilation angle against temperature for norite.

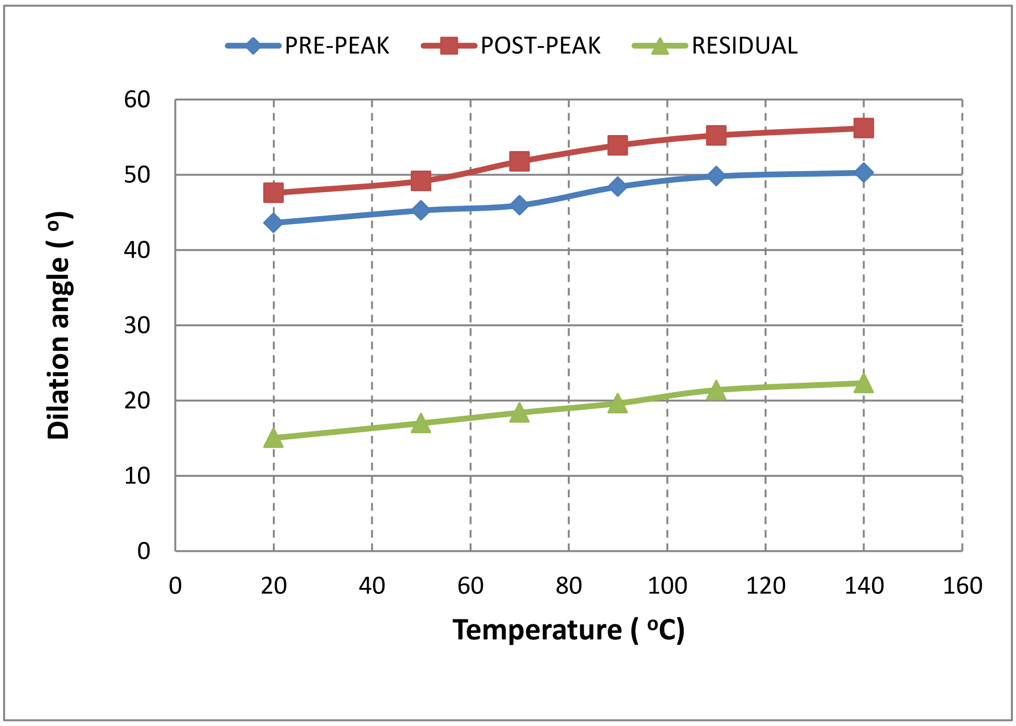

Figure A6 4: Dilation angle against temperature for vari-textured anorthosite

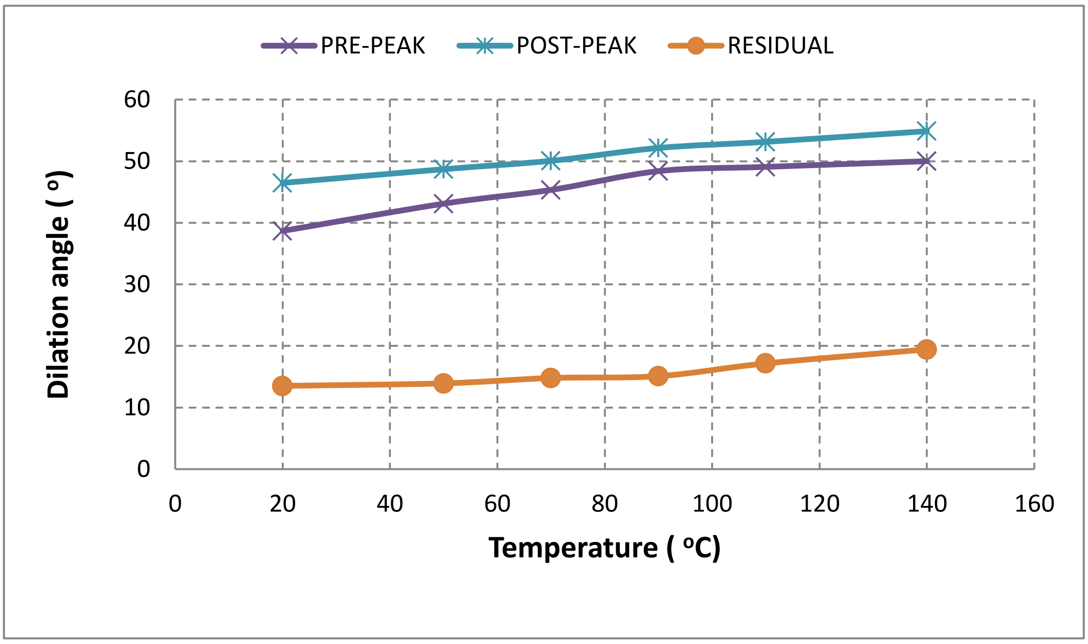

Figure A6 5: Dilation angle against temperature for leuconorite

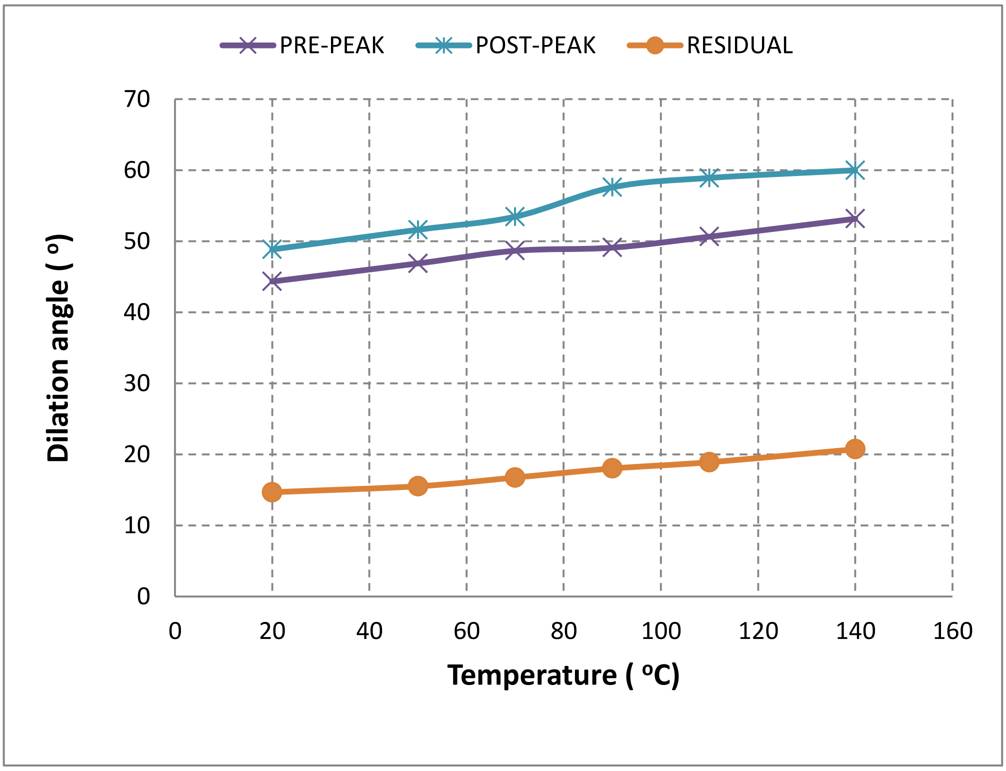

Figure A6 6: Plot of dilation angle against temperature for anorthosite-chromitite.